20. T. Imanura, MN 9002A Standard optical attenuator, *Anritsu Tech. Rev.* **14**:32-41 (1991).
21. C. F. Varley, On a new method of testing electronic resistance, *Math. Phys. Sect. Br. Assoc. Adr. Sci.* 14–15 (1866).
22. M. L. Morgan and J. C. Riley, Calibration of a Kelvin–Varley standard divider, *IRE Trans.* **I-9**(1):243–273 (1960).
23. A. F. Dunn, Calibration of a Kelvin–Varley voltage divider, *IEEE Trans. Instrum. Meas.* **IM-3**:129–139 (1964).
24. J. J. Hill and A. P. Miller, A seven-decade adjustable-ratio-inductively coupled voltage divider with 0.1 part per million accuracy, *Proc. IEE* **109**:157–162 (1962).
25. S. Avramov et al., Automatic inductance voltage divider bridge for operation from 10 Hz to 100 kHz, *IEEE Trans. Instrum. Meas.* **42**:131–135 (1993).
26. R. Yell, NPL MK 3 WBCO attenuator, *IEEE Trans. Instrum. Meas.* **IM-27**:388–391 (1978).
27. R. Yell, Developments in waveguide below cutoff attenuators at NPL, *IEE Colloq. Digest* **49**:1/1–1/5 (1981).
28. H. Bayer, Consideration of a rectangular waveguide below cutoff piston attenuator as calculable broad-band attenuation standard between 1 MHz and 2.6 GHz, *IEEE Trans. Instrum. Meas.* **IM-29**:467–471 (1980).
29. F. L. Warner, D. O. Watton, and P. Herman, A very accurate X-band rotary vane attenuator with an absolute digital angular measurement system, *IEEE Trans. Instrum. Meas.* **IM-21**:446–450 (1972).
30. W. E. Little, W. Larson, and B. J. Kinder, Rotary vane attenuator with an optical readout, *J. Res. NBS* **75C**:1–5 (1971).
31. W. Larson, *The Rotary Vane Attenuator as an Interlaboratory Standard*, NBS Monograph 144, U.S. Government Printing Office, Washington DC, Nov. 1975.
32. H. Bayer, F. Warner, and R. Yell, Attenuation and ratio-national standards, *Proc. IEEE* **74**:46–59 (1986).
33. T. Imamura, MN9002 Standard optical attenuator, *Annitsu Tech. Rev.* **14**:32–41 (1991).
34. G. F. Engen and R. W. Beatty, Microwave attenuation measurements with accuracies from 0.0001 to 0.06 dB over a range of 0.01 to 50 dB, *J. Res. NBS* **64C**:139–145 (1960).
35. H. Bayer, An error analysis for the RF-attenuation measuring equipment of the PTB applying the power method, *Metrologia*, **11**:43–51 (1975).
36. D. L. Hollway and F. P. Kelly, A standard attenuator and the precise measurement of attenuation, *IEEE Trans. Instrum. Meas.* **IM-13**:33–44 (1964).
37. F. L. Warner, P. Herman, and P. Cumming, Recent improvements to the UK national microwave attenuation standards, *IEEE Trans. Instrum. Meas.* **IM-32**(1):33–37 (1983).
38. F. K. Weinert, High performance microwave ratio meter employs parallel if complex vector substitution, *Microwave J.* **24**:51–85 (1981).
39. Hewlett-Packard, *Understanding the Fundamental Principles of Vector Network Analysis*, HP Application Note 1287-1, 1997; *Exploring the Architectures of Network Analyzers*, HP Application Note 1287-2, 1997; *Applying Error Correction to Network Analyzer Measurement*, HP Application Note 1287-3, 1997.
40. G. F. Engen, *Microwave Circuit Theory and Foundations of Microwave Metrology*, IEE Electrical Measurement Series Vol. 9, Peter Peregrinus, London, 1992.
41. O. D. D. Soares, ed., Trends in optical fibre metrology, *Part VI: Optical Fibre Characterisation, Calibration Standards*, Fibre Characterization and Measurement, pp. 353–397; NATO ASI Series E, Applied Sciences, Kluwer, Dordrecht, 1995, Vol. 285.
42. C. Hentschel, *Fibre Optics Handbook*, Hewlett-Packard, HP 13100-5952-9654, Hewlitt-Packard, Boblingen, Germany, 1989.
43. International Electrotechnical Commission, *Optical Fibres—Part 1: Generic Specification*, IEC 793-1 (11/92).
44. International Telecommunications Union, *Definition and Test Methods for the Relevant Parameters of Single Mode Fibres*, ITU-T G 650 (03/93).
45. T. Jones, *Attenuation and Cut-off Wavelength Measurement*, National Physical Laboratory, Optical Fibre Measurement Course, April 27–28, 1993.
46. D. J. Ives and B. Walker, *Optical Time Domain Reflectometry*, National Physical Laboratory, Optical Fibre Measurement Course, April 27–28, 1993.
47. International Organization for Standardization, *Guide to the Expression of Uncertainty in Measurement*, 1st ed., International Organization for Standardization, Geneva, 1993; corrected and reprinted 1995.
48. European Cooperation for Accreditation of Laboratories, *Expression of the Uncertainty of Measurement in Calibration*, EAL-R2, 1st ed., April 1997; *Examples*, EAL-R2-S1, 1st ed., Nov. 1997.
49. I. A. Harris and F. L. Warner, Re-examination of mismatch uncertainty when measuring microwave power and attenuation, *IEE Proc. H* **128**(1):35–41 (1981).

ATTENUATORS

RAJI SUNDARARAJN
EDWARD PETERSON
ROBERT NOWLIN
Arizona State University East
Mesa, Arizona

Attenuators are linear, passive, or active networks or devices that attenuate electrical or microwave signals, such as voltages or currents, in a system by a predetermined ratio. They may be in the form of transmission-line, stripline, or waveguide components. Attenuation is usually expressed as the ratio of input power ($P_{\rm in}$) to output power ($P_{\rm out}$), in decibels (dB), as

$$\text{Attenuation}\,(A) = 10\,\log_{10}\frac{P_{\rm in}}{P_{\rm out}} = 20\,\log\frac{E_{\rm in}}{E_{\rm out}} = 20\,\log\frac{E_1}{E_2} \tag{1}$$

This is derived from the standard definition of attenuation in Nepers (Np), as

$$\text{Attenuation}\,(A) = \alpha\Delta x = -\ln\frac{|E_2|}{|E_1|} \tag{2}$$

where α is attenuation constant (Np/m) and Δx is the distance between the voltages of interest (E_1 and E_2).

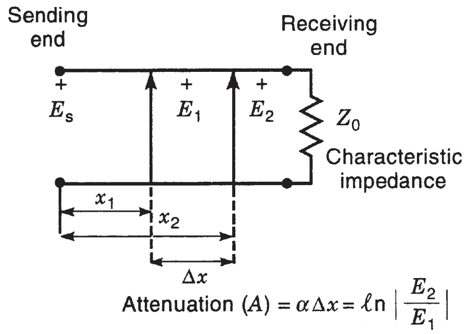

Figure 1. Concept and definition of attenuation.

Figure 1 illustrates this concept. The relation between Np and dB is

$$1\text{Np} = 8.686\,\text{dB} \tag{3}$$

Here the load and source are matched to the characteristic impedance. The decibels are converted to the attenuation ratio as follows: $P_{\text{in}}/P_{\text{out}} = \log_{10}^{-1} \text{dB}/10$ or $V_{\text{in}}/V_{\text{out}} = \log_{10}^{-1} \text{dB}/20$.

The most commonly used method in attenuators is to place resistors at the center of an electric field. Due to the electric field, there is current induced, resulting in ohmic loss.

1. APPLICATION

There are many instances when it is necessary to reduce the value, or level, of electrical or microwave signals (such as voltages and currents) by a fixed amount to allow the rest of the system to work properly. Attenuators are used for this purpose. For example, in turning down the volume on a radio, we make use of a variable attenuator to reduce the signal. Almost all electronic instruments use attenuators to allow for the measurement of a wide range of voltage and current values, such as voltmeters, oscilloscopes, and other electronic instruments. Thus, the various applications in which attenuators are used include the following:

- To reduce signal levels to prevent overloading
- To match source and load impedances to reduce their interaction
- To measure loss or gain of two-port devices
- To provide isolation between circuit components, or circuits or instruments so as to reduce interaction among them
- To extend the dynamic range of equipment and prevent burnout or overloading equipment

2. TYPES

There are various types of attenuators based on the nature of circuit elements used, type of configuration, and kind of adjustment. They are as follows:

Figure 2. Fixed coaxial attenuator. (Courtesy of Weinschel Associates.)

- Passive and active attenuators
- Absorptive and reflective attenuators
- Fixed and variable attenuators

A fixed attenuator is used when the attenuation is constant. Variable attenuators have varying attenuation, using varying resistances for instance. The variability can be in steps or continuous, obtained either manually or programmably. There are also electronically variable attenuators. They are reversible, except in special cases, such as a high-power attenuator. They are linear, resistive, or reactive, and are normally symmetric in impedance. They include waveguide, coaxial, and striplines, as well as calibrated and uncalibrated versions. Figures 2–4 show fixed, manual step, and continuously variable commercial attenuators, respectively.

Based on their usage, IEEE Std 474 classifies them as

Class I	Standard
Class II	Precision
Class III	General-purpose
Class IV	Utility

Typical commercial attenuators are listed below:

WA 1 (0–12.4 GHz), WA 2 (0–3 GHz), coaxial, fixed attenuators: 1–60 dB; 5 W av./1 kW peak

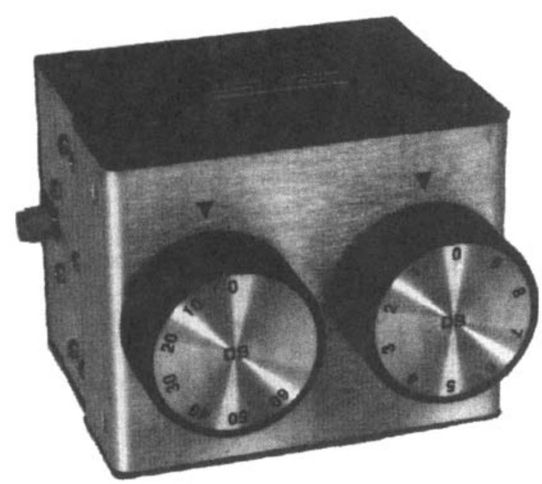

Figure 3. Manual step attenuator. (Courtesy of Weinschel Associates.)

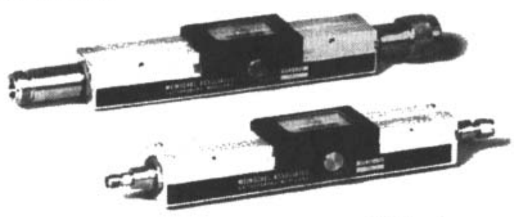

Figure 4. Continuously variable attenuator. (Courtesy of Weinschel Associates.)

WA 115A manual step attenuators: 0–18 GHz, 0–9 dB, 1-dB steps

VA/02/100 continuously variable attenuators, resistive, 0–2 GHz, 5 W av./0.5 kW peak

HP 84904L programmable step attenuator, direct current (DC) to 40 GHz, 0–11 dB, 1-dB steps

HP 84906 K programmable step attenuator, DC to 26.5 GHz, 0–90 dB, 10-dB steps

HP 84904L programmable step attenuator, DC to 40 GHz, 0–70 dB, 10-dB steps

HP 8495B manual step attenuator, DC to 18 GHz, 0–70 dB, 10-dB steps

HP 355F programmable step attenuator, DC to 1 GHz, 0–120 dB, 10-dB steps

HP 8493A coaxial fixed attenuator, DC to 12.4 GHz

Based on their utility, military attenuators are classified as:

Class I	For use as a primary standard
Class II	For use as a secondary standard, and in lab and precision test equipment A—with lumped constant or distributed shunt and series elements B—with lossy-line pads
Class III	For use in general field equipment
Class IV	For use in equipment where precision and stability are secondary considerations

Typical military specifications for fixed coaxial attenuators are as follows:

Mil-A-3933/1: attenuators, fixed, coaxial line, DC to 3 GHz, class IIA, low power

Mil-A-3933/2: attenuators, fixed, coaxial line, 1–4 GHz, class IIB, medium power

Mil-A-3933/10: attenuators, fixed, coaxial line, DC to 18 GHz, class III, medium power

Mil-A-3933/26: attenuators, fixed, coaxial line, 0.4–18 GHz, class IV low power

3. SPECIFICATIONS

To specify an attenuator, the purpose of the attenuator should be known. Attenuators are used to provide protection, reduce power, and extend the dynamic range of the test equipment. In choosing an attenuator, the frequency range of operation should be considered since the accuracy depends on the frequency. Attenuation involves placing resistive material to absorb the signal's electric field. This means, there will always be some reflection. So, attenuators must be designed to minimize reflection. This is quantified in terms of voltage standing-wave ratio (VSWR). Another factor to be considered is the insertion loss, which is the ratio of power levels with and without the component insertion. If it is a variable step attenuator, the step size is to be known. Thus, the parameters available in the specs are as follows:

dB rating

VSWR

Accuracy

Power rating

Stepsize (if variable)

Frequency band

Degree of stability (measured by the change in attenuation due to temperature, humidity, frequency, and power level variations)

Characteristic impedance of attenuator

Repeatability

Life

Degree of resolution (difference between actual attenuation and measured value)

The definitions of various parameters used in selecting attenuators are given below.

3.1. Electrical Parameters and Definitions (from MIL-HDBK-216)

Attenuation. A general transmission term used to indicate a decrease in signal magnitude. This decrease in power is commonly expressed in decibels (dB) as

$$\text{Attenuation } (A) = 10 \log_{10} \frac{P_{\text{in}}}{P_{\text{out}}}$$

Deviation of Attenuation from Normal. Difference in actual attenuation from the nominal value at 23°C and an input power of 10 mW at a specified reference frequency or frequency range. When used in a frequency range, it involves the frequency sensitivity.

Frequency Sensitivity. This is the peak-to-peak variation in the loss of the attenuator through the specified frequency range.

Frequency Range. Range of frequency over which the accuracy of attenuator is specified.

Insertion Loss. Amount of power loss due to the insertion of the attenuator in the transmission system. It is expressed as a ratio of the power delivered to that part of the system following the attenuator, before and after the insertion.

Characteristic Insertion Loss. This is the insertion loss in a transmission line or waveguide that is reflectionless in both directions from the inserted attenuator.

Power-Handling Capabilities. Maximum power that can be applied to the attenuator under specified conditions and durations without producing a permanent change in the performance characteristics that would be outside of specification limits.

Power Sensitivity. This is the temporary variation in attenuation (dB/W) under steady-state conditions when the input power is varied from 10 mW to maximum input power.

Stability of Attenuation. Capability of attenuator to retain its parameters when subjected to various environmental conditions.

Operating Temperature Range. Temperature range of the attenuator can be operated with maximum input power.

Temperature Sensitivity. Temperature variation in attenuation [dB/(dB × °C)] over the operating range.

Input VSWR. This is the level of reflected signal created at the attenuator input when the output is terminated with a load with the same characteristic impedance as the source.

Output VSWR. This is the level of reflected signal created at the attenuator output when the input is terminated with a load with the same characteristic impedance as the source.

4. PASSIVE ATTENUATORS

4.1. Resistance Networks for Attenuators

Typically T, pi, or L designs are used for attenuators. Figure 5 shows four commonly used symmetric (input and output resistors of equal value) configurations. The formulas for the resistance values in ohms for these pads when the characteristic resistance $R_0 = 1\,\Omega$ are given

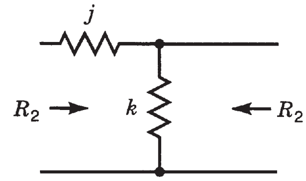

Figure 6. Unsymmetric matching L attenuator.

below. If R_0 is other than $1\,\Omega$, multiply each of the resistance values (a, b, c, $1/a$, $1/b$, and $1/c$) by R_0, where

$$a = \frac{10^{\mathrm{dB}/20} - 1}{10^{\mathrm{dB}/20} + 1} \tag{4}$$

$$b = \frac{2 \times 10^{\mathrm{dB}/20}}{10^{\mathrm{dB}/10} - 1} \tag{5}$$

$$c = (10^{\mathrm{dB}/20} - 1) \tag{6}$$

Simple wirewound resistors are used in audio applications. Nonreactive wirewound resistors, such as mica card, Aryton–Perry winding, woven resistors are used for high frequencies. For coaxial applications (over 26.5 GHz), thin-film resistors are used. For higher frequencies, distributive resistive films, such as nichrome alloy film, on a high-quality ceramic substrate, such as alumina or sapphire, is used. An unsymmetrical pad is shown in Fig. 6, and the formulas for this pad are

$$j = \frac{R_1 - kR_2}{k + R_2} \tag{7}$$

$$k = \left[\frac{R_1 R_2^2}{(R_1 - R_2)}\right]^{1/2} \quad \text{where } R_1 > R_2 \tag{8}$$

$$\text{Minimum loss (dB)} = 20 \log\left\{\left[\frac{(R_1 - R_2)}{R_2}\right]^{1/2} + \left(\frac{R_1}{R_2}\right)^{1/2}\right\} \tag{9}$$

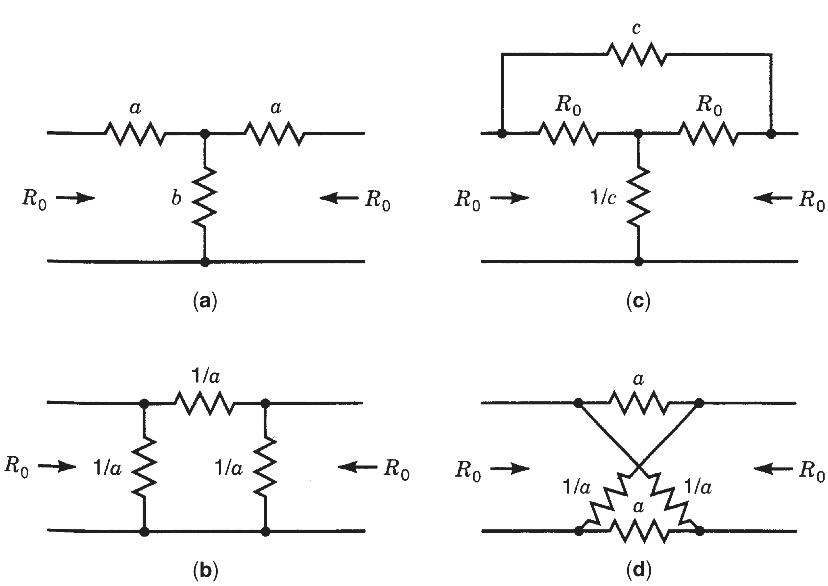

Figure 5. Symmetric pads with matched impedances: (a) T pad; (b) pi pad; (c) bridged T pad; (d) balanced pad.

Table 1. Resistance Values for Attenuator Pads When $R_0 = 1\,\Omega$[a]

	T Pad		Pi Pad		Bridged T Pad		Balanced Pad	
	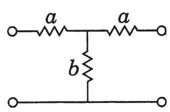		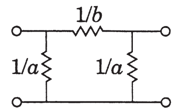		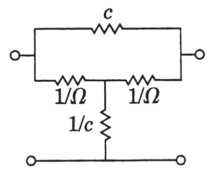		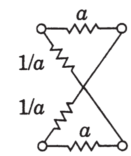	
dB[b]	a	b	$1/b$	$1/a$	c	$1/c$	a	$1/a$
0.1	0.0057567	86.853	0.011514	173.71	0.011580	86.356	0.0057567	173.71
0.2	0.011513	43.424	0.023029	86.859	0.023294	42.930	0.011513	86.859
0.3	0.017268	28.947	0.034546	57.910	0.035143	28.455	0.017268	57.910
0.4	0.023022	21.707	0.046068	43.438	0.047128	21.219	0.023022	43.438
0.5	0.028775	17.362	0.057597	34.753	0.059254	16.877	0.028775	34.753
0.6	0.034525	14.465	0.069132	28.965	0.071519	13.982	0.034525	28.965
0.7	0.040274	12.395	0.080678	24.830	0.083927	11.915	0.040274	24.830
0.8	0.046019	10.842	0.092234	21.730	0.096478	10.365	0.046019	21.730
0.9	0.051762	9.6337	0.10380	19.319	0.10918	9.1596	0.051762	19.319
1.0	0.057501	8.6668	0.11538	17.391	0.12202	8.1954	0.057501	17.391
2.0	0.11462	4.3048	0.23230	8.7242	0.25893	3.8621	0.11462	8.7242
3.0	0.17100	2.8385	0.35230	5.8481	0.41254	2.4240	0.17100	5.8481
4.0	0.22627	2.0966	0.47697	4.4194	0.58489	1.7097	0.22627	4.4194
5.0	0.28013	1.6448	0.60797	3.5698	0.77828	1.2849	0.28013	3.5698
6.0	0.33228	1.3386	0.74704	3.0095	0.99526	1.0048	0.33228	3.0095
7.0	0.38248	1.1160	0.89604	2.6145	1.2387	0.80727	0.38248	2.6145
8.0	0.43051	0.94617	1.0569	2.3229	1.5119	0.66143	0.43051	2.3229
9.0	0.47622	0.81183	1.2318	2.0999	1.8184	0.54994	0.47622	2.0999
10.0	0.51949	70.273[c]	1.4230	1.9250	2.1623	46.248[c]	0.51949	1.9250
20.0	0.81818	20.202[c]	4.9500	1.2222	9.0000	11.111[c]	0.81818	1.2222
30.0	0.93869	6330.9[c]	15.796	1.0653	30.623	3265.5[c]	0.93869	1.0653
40.0	0.980198	2000.2[c]	49.995	1.0202	99.000	1010.1[c]	0.980198	1.0202
50.0	0.99370	632.46[c]	158.11	1.0063	315.23	317.23[c]	0.99370	1.0063
60.0	0.99800	200.00[c]	500.00	1.0020	999.00	100.10[c]	0.99800	1.0020
70.0	0.99937	63.246[c]	1581.1	1.0006	3161.3	31.633[c]	0.99937	1.0006
80.0	0.99980	20.000[c]	5000.0	1.0002	9999.0	10.001[c]	0.99980	1.0002
90.0	0.99994	6.3246[c]	15.811	1.0001	31.622	3.1633[c]	0.99994	1.0001
100.0	1.0000	2.0000[c]	50.000	1.0000	99.999	1.0000[c]	1.0000	1.0000

[a] If $R_0 \neq 1\,\Omega$, multiply all values by R_0. (From Ref. data for *Radio Engineers*, 1985.)
[b] For other decibel values, use formulas in text.
[c] These values have been multiplied by 10^3.

Typical values for the pads in Fig. 5 are shown in Table 1, and those of Fig. 6 are shown in Table 2.

For a broadband match between impedances R_1 and R_2, use the minimum-loss L pad (Fig. 6).

4.2. Power Dissipation within a T Pad

Table 3 lists values of power dissipation within a T pad. The values are for an input of 1 W; for other input powers, multiply the values by the input power.

5. INSERTION LOSS

An attenuator is used to introduce attenuation between a source and a load. Due to the introduction of the attenuator, there is change in the current. This loss is designated as insertion loss, which depends on the configuration. Usually, the load and source impedances are matched. Figure 7 illustrates this concept. If I_{L0} is the load current without the attenuator pad and I_L is the current with the attenuator pad, then the ratio I_L/I_{L0} is called the *insertion loss*, one of the parameters of the attenuates. Figure 7a shows the source and load connected without an attenuator, and Fig. 7b shows the same system with an attenuator. (The quantities I_L, R_{in}, and R_{out} depend on the attenuator configuration.) The quantities insertion loss (I_L), input resistance (R_{in}), and output resistance (R_{out}) depend on the attenuator configuration. The value of each of the three resistors of the T (Fig. 8) and pi (Fig. 9) attenuators can be chosen independently of others. This enables the three-design criteria of input resistance, output resistance, and insertion loss to be met. In many situations, the only function of the pad is to provide matching between source and load; and although attenua-

Table 2. Resistance Values and Attenuation for L Pad[a]

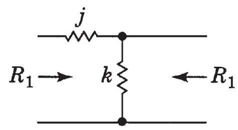

R_1/R_2	j	k	dB
20.0	19.49	1.026	18.92
16.0	15.49	1.033	17.92
12.0	11.49	1.044	16.63
10.0	9.486	1.054	15.79
8.0	7.484	1.069	14.77
6.0	5.478	1.095	13.42
5.0	4.472	1.118	12.54
4.0	3.469	1.155	11.44
3.0	2.449	1.225	9.96
2.4	1.833	1.310	8.73
2.0	1.414	1.414	7.66
1.6	0.9798	1.633	6.19
1.2	0.4898	2.449	3.77
1.0	0	∞	0

[a]For $R_2 = 1\,\Omega$ and $R_1 > R_2$. If $R_2 \neq 1\,\Omega$, multiply values by R_2. For ratios not in the table, use the formulas in the text. (From Ref. data for *Radio Engineers*, 1985.)
Examples of use of table:
If $R_1 = 50\,\Omega$ and $R_2 = 25\,\Omega$, then $R_1/R_2 = 2.0$, and $j = k = 1.414 \times 25\,\Omega = 35.35\,\Omega$.
If $R_1/R_2 = 1.0$, minimum loss $= 0$ dB.
For $R_1/R_2 = 2.0$, the insertion loss with the use of j and k for matching is 7.66 dB above that for $R_1/R_2 = 0$.

tion will be introduced, this may not be a critical design parameter. This allows a simpler type of pad to be designed, requiring only two resistors; it is known as an "L pad."

Figure 10 shows an L attenuator, which can be derived from either a T or a pi attenuator, simply by removing one of the resistors. As shown, different configurations are required depending on whether $R_S > R_L$ or $R_S < R_L$.

5.1. T Attenuator Insertion Loss

The T attenuator contains resistors R_1, R_2, and R_3; these form a T configuration, as shown in Fig. 6. Insertion loss is usually measured in dB, defined as $I_L(\text{dB}) = -20 \log I_L$ or $|20 \log I_L|$, the amount of attenuation required. The insertion loss I_L is given as

$$I_L(\text{dB}) = \frac{I_L}{I_{L0}} = \frac{R_3(R_S + R_L)}{(R_S + R_1 + R_3)(R_2 + R_3 + R_L) - R_3^2} \tag{10}$$

The input and the output of resistances of the attenuator are given by

$$R_{in} = R_1 + \frac{R_3(R_2 + R_L)}{R_2 + R_3 + R_L} \tag{11}$$

and

$$R_{out} = R_2 + \frac{R_3(R_1 + R_S)}{R_1 + R_3 + R_S} \tag{12}$$

Table 3. Power Dissipation in T Pad[a]

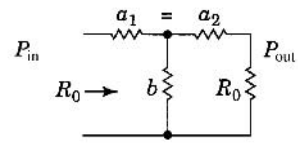

dB	Watts, Input Series Resistor	Watts, Shunt Resistor	Watts, Output Series Resistor
0.1	0.00576	0.0112	0.005625
0.3	0.0173	0.0334	0.016113
0.5	0.0288	0.0543	0.025643
0.7	0.0403	0.0743	0.034279
0.9	0.0518	0.0933	0.0421
1.0	0.0575	0.1023	0.0456
1.2	0.0690	0.120	0.0523
1.4	0.0804	0.11368	0.0582
1.6	0.0918	0.1525	0.0635
1.8	0.103	0.1672	0.0679
2.0	0.114	0.1808	0.0718
2.2	0.126	0.1953	0.0758
2.4	0.137	0.2075	0.0787
2.6	0.149	0.2205	0.0818
2.8	0.160	0.232	0.0839
3.0	0.170998	0.242114	0.085698
3.2	0.182	0.2515	0.0870
3.4	0.193	0.2605	0.0882
3.6	0.204	0.2695	0.0890
3.8	0.215	0.2775	0.0897
4.0	0.226	0.285	0.0898
5	0.280	0.3145	0.0884
6	0.332	0.332	0.0833
7	0.382	0.341	0.0761
8	0.430	0.343	0.0681
9	0.476218	0.33794	0.0599527
10	0.519	0.328	0.0519
12	0.598	0.3005	0.0377
14	0.667	0.266	0.0266
16	0.726386	0.23036	0.0182460
18	0.776	0.1955	0.0123
20	0.818	0.1635	0.0100
30	0.938	0.0593	0.0010
40	0.980	0.0196	0.0001

[a]For 1 W-input and matched termination. If input $\neq$ 1 W, multiply values by P_{in}. (From Ref. data for *Radio Engineers*, 1985.)

In many cases, the attenuator also has to match the load and the source impedance. In this case, $R_1 = R_2 = R$ and $R_{in} = R_{out} = R_0$. Thus

$$R_0 = R + \frac{R_3(R + R_0)}{(R_3 + R + R_0)} \tag{13}$$

and the insertion loss is given by

$$I_L = \frac{R_3}{R_3 + R + R_0} \tag{14}$$

and

$$R = R_0 \frac{1 - I_L}{1 + I_L} \tag{15}$$

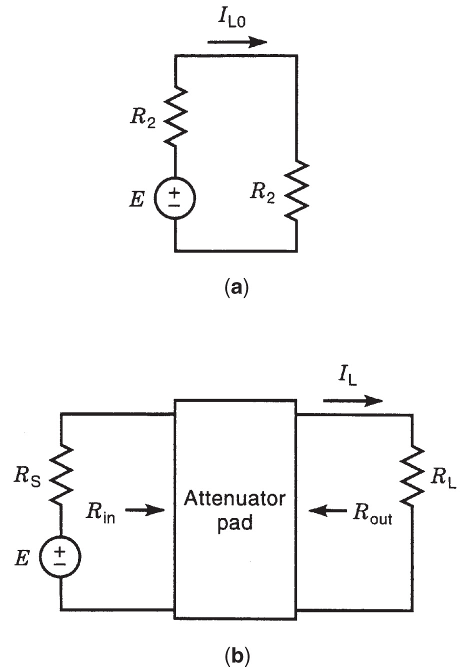

Figure 7. Definition of characteristic insertion loss: (a) original setup without attenuator; (b) original setup with attenuator between source and load.

and

$$R_3 = \frac{2R_0 I_L}{1-(I_L)^2} \tag{16}$$

Example 1 (T Attenuator). A T-type attenuator is required to provide 3 × 0 dB insertion loss and to match 50 Ω input and output. Find the resistor values,

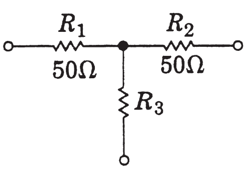

$$3\,\text{dB} = -20 \log I_L$$
$$I_L = 10^{(-3/20)} = 0.708$$

using the following equations:

$$R = R_0 \frac{1-I_L}{1+I_L} = 50\left(\frac{1-0.708}{1+0.708}\right) = 8.55\ \Omega$$

$$R_3 = \frac{2R_0 I_L}{1-(I_L)^2} = \frac{2 \times 50 \times 0.708}{1-(0.708)^2} = 141.6\,\Omega$$

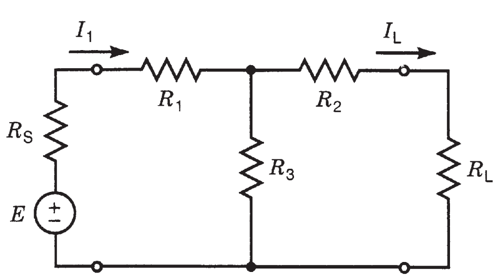

Figure 8. T attenuator configuration.

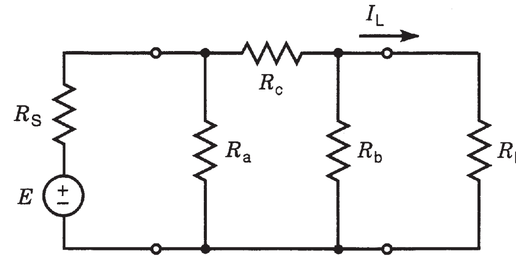

Figure 9. Pi attenuator configuration.

Check:

$$I_L = \frac{R_3}{R_3 + R + R_0} = \frac{141.6}{141.6 + 8.55 + 50} = 0.708$$

5.1.1. The Pi Attenuator Insertion Loss. Figure 9 shows a pi attenuator formed by resistors R_a, R_b, and R_c. The insertion loss and conductances G_{in} and G_{out} are given by

$$I_L = G_c \frac{G_S + G_L}{(G_S + G_a + G_c(G_b + G_c + G_L) - G_c^2} \tag{17}$$

$$G_{in} = G_a + \frac{G_c(G_b + G_L)}{G_b + G_c + G_L} \tag{18}$$

$$G_{out} = G_b + \frac{G_c(G_a + G_S)}{G_a + G_c + G_S} \tag{19}$$

where $G = 1/R$; thus $G_L = 1/R_L$ and so on.

The same pi attenuator can be realized using a T attenuator with R_1, R_2, and R_3 values using the Y–Δ

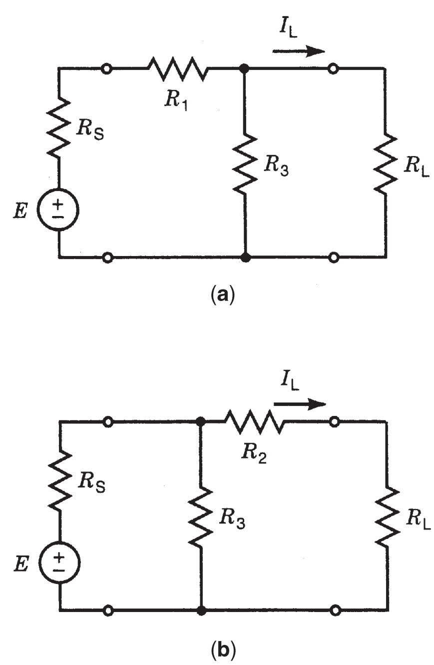

Figure 10. L attenuator configuration:(a) $R_s < R_I$; (b) $R_s > R_I$.

transformation:

$$R_a = \frac{R_1R_2 + R_1R_3 + R_2R_3}{R_2} \tag{20}$$

$$R_b = R_a \frac{R_2}{R_1} \tag{21}$$

$$R_c = R_a \frac{R_2}{R_3} \tag{22}$$

The selection between pi and T is based on the value of resistors that can be used in practice. With matching source and load impedances, the values of the pi attenuator are

$$R_a = R_b = R_0 \frac{1 + I_L}{1 - I_L} \tag{23}$$

and

$$R_c = R_0 \frac{1 - (I_L)^2}{2I_L} \tag{24}$$

Example 2 (Pi Attenuator). Repeat Example 1 using a pi attenuator

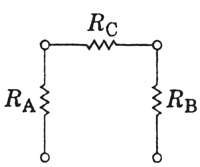

$$R_L\,(\text{dB}) = 3 = -20 \log I_L$$
$$I_L = 10^{(-3/20)} = 0.708$$

using the following equations:

$$R_A = R_B = R_0 \frac{1 + I_L}{1 - I_L} = 50\left(\frac{1 + 0.708}{1 - 0.708}\right) = 292.46\,\Omega$$

$$R_C = R_0\left(\frac{1 - (I_C)^2}{2I_L}\right) = 50\left(\frac{1 - (0.708)^2}{2 \times 0.708}\right) = 17.61\,\Omega$$

5.1.2. The L Attenuator Insertion Loss. An L attenuator can be derived from a T or pi attenuator by removing one resistor. As shown in Fig. 10, two configurations are obtained depending on $R_S > R_L$ or $R_S < R_L$. Simple circuit theory shows that for $R_S > R_L$, we have

$$R_S = R_{in} = R_1 + \frac{R_3R_L}{R_3 + R_L} \tag{25}$$

and

$$R_L = R_{out} = \frac{R_3(R_1 + R_S)}{R_3 + R_1 + R_S} \tag{26}$$

from which it can be shown that

$$R_1 = \sqrt{R_S(R_S - R_L)} \tag{27}$$

and

$$R_3 = \frac{R_S^2 - R_1^2}{R_1} \tag{28}$$

and when we put $R_2 = 0$, the insertion loss is calculated as

$$I_L = \frac{R_3(R_S + R_L)}{(R_S + R_1 + R_3)(R_3 + R_L) - R_3^2} \tag{29}$$

Example 3. Design an L attenuator to match a 300-Ω source to a 50-Ω load and determine insertion loss. Here $R_S > R_L$ using the following equation:

$$R_1 = \sqrt{R_S(R_S - R_L)} = \sqrt{300(300 - 50)}$$
$$= \sqrt{300 \times 250} = 273.86\,\Omega$$

Using the following equation:

$$R_3 = \frac{R_S^2 - R_1^2}{R_1} = \frac{300^2 - 273.86^2}{273.86} = 54.775\,\Omega$$

$$R_L = \frac{R_3(R_S + R_L)}{(R_S + R_1 + R_3)}(R_3 + R_L) - R_3^2$$

$$= \frac{54.775\,(300 + 50)}{(300 + 273.86 + 54.775)(54.775 + 50) - (54.775)^2}$$
$$= 0.305$$

$$R_L(\text{dB}) = -20 \log 0.305 = 10.3\,\text{dB}$$

For $R_S < R_1$, we have

$$R_{in} = \frac{R_3(R_2 + R_L)}{R_2 + R_3 + R_L} \tag{30}$$

and

$$R_{out} = R_2 + \frac{R_3R_S}{R_3 + R_S} \tag{31}$$

and

$$R_2 = \sqrt{R_L(R_L - R_S)} \tag{32}$$

and

$$R_3 = \frac{R_L^2 - R_2^2}{R_2} \tag{33}$$

The corresponding insertion loss is

$$I_L = \frac{R_3(R_S + R_L)}{(R_S + R_3)(R_2 + R_3 - R_L) - R_3^2} \tag{34}$$

Example 4. Design an L attenuator to match 50-Ω source to 75-Ω load and determine the insertion loss $R_S < R_L$, using the following equation:

$$R_2 = \sqrt{R_L(R_L - R_S)} = \sqrt{75\,(75 - 50)} = 43.3\,\Omega$$

using the following equations:

$$R_3 = \frac{R_L^2 - R_2^2}{R_2} = \frac{75^2 - 43.3^2}{43.3} = 86.6\,\Omega$$

$$R_L = \frac{R_3(R_S + R_L)}{(R_S + R_3)(R_2 + R_3 + R_L) - R_3^2}$$

$$= 0.0123 = 38.2\,\text{dB}$$

6. FIXED ATTENUATORS

Fixed attenuators, commonly known as "pads," reduce the input signal power by a fixed amount, such as 3, 10, and 50 dB. For example, an input signal of 10 dBm (10 mW) passing through a 3-dB fixed attenuator will exit with a power of 10 dBm − 3 dB = 7 dBm (5 mW). Figure 2 shows a fixed coaxial commercial attenuator. A typical datasheet for a fixed coaxial attenuator is as follows (courtesy of Weinschel Associates):

Frequency	0–3 GHz
Attenuation	50 dB
Accuracy	±0.10 dB (DC) ±0.15 dB (0–2 GHz) ±0.13 dB (0–3 GHz)
VSWR	1.15 (0–1 GHz) 1.20 (1–3 GHz)
Input power	1 W av., 1 kW peak at −30°–70°C
Connectors	Type N; St. St.; m, f
Length	68 mm (2.7 in.)
Diameter	210 mm (0.83 in.)
Weight	100 g (3.6 oz)
Power sensitivity	<0.005 dB/dB × W; bidirectional in power
Temperature stability	<0.0004 dB/dB × °C

6.1. Applications

Fixed attenuators are used in numerous applications. In general, they can be classified into two distinct categories:

1. Reduction in signal level
2. Impedance matching of a source and a load

Those in the first category are used in the following situations:

- Operation of a detector in its square-law range for most efficient operations.
- Testing of devices in their small signal range.
- Reduction of a high-power signal to a level compatible with sensitive power measuring equipment, such as power sensors and thermistor mounts.

Those in the second category are used in the following situations:

- Reduction of signal variations as a function of frequency. The variations here are caused by a high VSWR. The attenuator provides a reduction in these variations and a better match.
- Reduction in frequency pulling (changing the source frequency by changing the load) of solid-state sources by high reflection loads.

6.2. Types

Based on construction, fixed attenuators are available in coaxial, waveguide, and stripline configurations. The various types are:

1. Waveguide vane
2. Rotary vane (fixed)
3. Directional coupler
4. T or pi
5. Lossy line
6. Distributed resistive film

6.2.1. Coaxial Fixed Attenuators. T or pi configurations are most commonly used both at low and high frequencies. At low frequencies, normal wirewound resistors are used. At high frequencies, thin-film resistors are used. Figures 11 and 12 show T and pi fixed attenuators. Thin-film resistors designed for microwave frequencies are used in place of carbon resistors. These resistors employ a nichrome alloy film on a high-quality ceramic substrate to ensure a firmly bonded film with low-temperature coefficients. This type of construction makes the resistors extremely stable at high frequencies. The skin effect of these resistors is excellent, used extensively in the microwave applications.

The T and pi configurations are obtained by placing the resistors in series on the center conductor and in shunt, contacting both the center and outer conductor. Thus, the T configuration can be fabricated with one shunt flanked by two series resistors and the pi configuration, with one series flanked by two shunt resistors. The series resistors in the T and pi configurations have less than 1 W capacity, thereby severely limiting the use at high-power applications, unless an elaborate heatsinking is provided. Power attenuators usually have huge sinks to handle high-power applications.

6.2.2. Resistive Card Attenuator. In a fixed dissipative, waveguide-type resistive card attenuator, the card is bonded in place (Fig. 13). It is tapered at both ends to maintain a low-input and low-output VSWR over the useful waveguide band. Maximum attenuation per length is obtained when the card is parallel to the E field

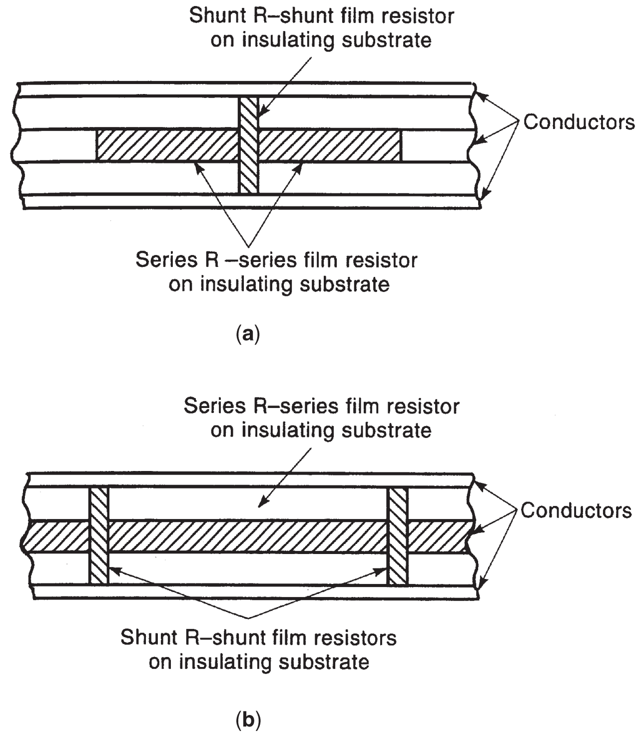

Figure 11. T/pi fixed attenuator configuration: (a) T section; (b) pi section.

and at the center, where the TE_{10} mode is maximum. The conductivity and the dimensions of the card are adjusted, by trial and error, to obtain the desired attenuation, which is a function of frequency. The attenuation increases with increase in frequency. In power applica-

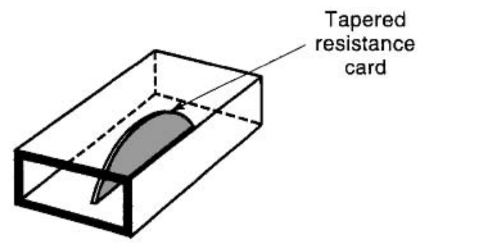

Figure 13. Fixed resistive card attenuator configuration.

tions, ceramic-type absorbing materials are used instead of a resistive card.

7. VARIABLE ATTENUATORS

A variable attenuator has a range, such as 0–20 dB or 0–100 dB. The variation can be continuous or in steps, obtained manually or programmably.

7.1. Step Attenuators

A series of fixed attenuators are mechanically arranged to offer discrete-step variation. The fixed attenuators are arranged in a rotatable drum or in a slab for switching between contacts. This arrangement provides discrete values of attenuation in each position and a high reliability factor. The step size can be 0.1, 1, or 10 dB. Stationary coaxial contacts provide the input and output of the device. These are used in applications requiring broadband flatness with low VSWR and satisfactory resettability over ranges from 0 to 120 dB. Their application range is DC to 18 GHz.

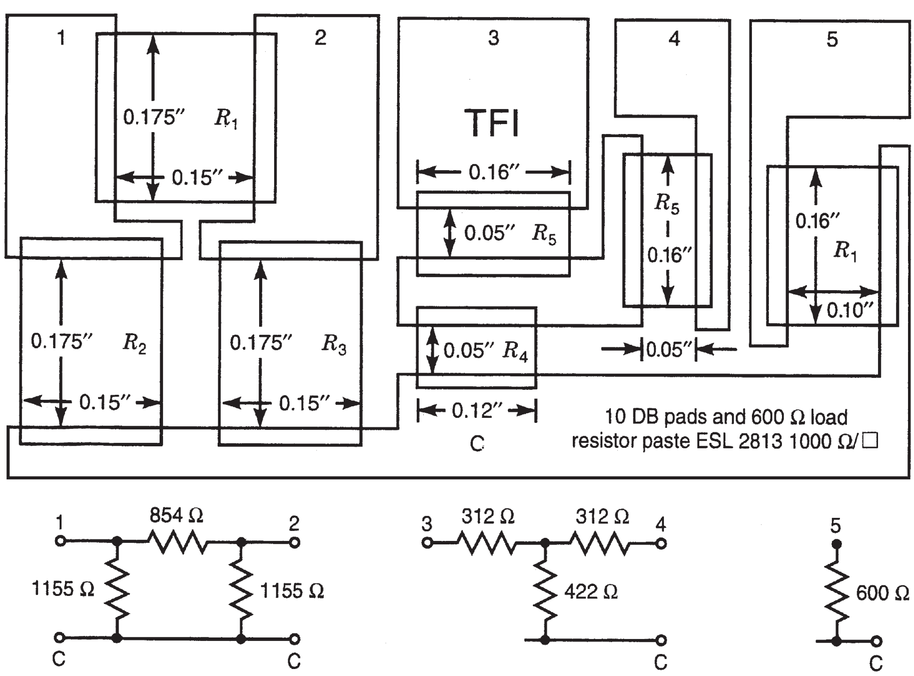

Figure 12. T/pi fixed-attenuator construction.

7.2. Manual Step Attenuators

Figure 3 shows a manual step attenuator. A typical datasheet looks as follows:

Frequency	0–4, 0–8, 0–12.4, 0–18 GHz
Attenuation	0–9, 0–60, 0–69
Stepsize	1, 10, 1 dB, respectively, for the range given above
VSWR	1.20, 1.25, 1.40, 1.50 for the frequency ranges given above 1.25, 1.30, 1.45, 1.60, for the frequency range given above
Connectors	N/SMA; St. St.
Height	83 mm (3.3 in.)
Depth	79 mm (3.1 in.) (excludes shaft and knob)
Width	65, 65, 118 mm (2.6, 2.6, 4.7 in.) for the three attenuation ranges given above

7.3. Continuously Variable Attenuators

Figure 4 shows a continuously variable attenuator. Typical specs are

Frequency	1–18 GHz, 1 W av./1 kW peak
Connectors	St. St., M, F; type N, SMA
Zero loss	Typically 0.5–1 dB
Attenuation	0–9, 0–60, 0–69 dB

The various types of continuously variable attenuators are

Lossy wall
Movable vane (Flap)
Rotary vane
Variable coupler
Absorptive type
Coaxial resistive film
Variable T
Waveguide below cutoff (piston)

7.4. Programmable and Solenoid Attenuators

7.4.1. Programmable. These are rapid switching attenuators with high accuracy and repeatability, useful for remote and computerized applications. Switching speeds can be as low as 30 ns. Two varieties of the programmable attenuators are the step-controlled and voltage-controlled types. The attenuation is varied by controlling the electrical signal applied to the attenuator. These signals can be in the form of either a biasing current or binary digit. The biasing can be pulses, square waves, or sine waves. A typical datasheet for coaxial programmable step attenuator is as follows:

Frequency	DC to 40 GHz
Attenuation	0–11 dB, in steps of 1 dB
Maximum VSWR	1.3–12.4 GHz 1.7–34 GHz 1.8–40 GHz
Insertion loss	0.8 dB + 0.04 GHz 0 dB setting
Repeatability	0.03 dB
Power rating average	1 W
Peak	50 W
Maximum pulse width	10 μs
Life	5 million cycles per section minimum

7.4.2. Solenoid. A typical datasheet would be as follows:

Voltage	20–30 V
Speed	$<$20 ms
Power	2.7 W
RF connectors	2.4 mm, F
Shipping weight	291 g (10.3 oz)

7.5. Lossy Wall Attenuator

Figure 14 shows lossy wall variable attenuator. It consists of a glass vane coated with a lossy material, such as aquadag or carbon. For maximum attenuation, the vane is placed in the center of the guide's wide dimension, where the electric field intensity is the maximum. A drive mechanism with a dial then shifts the vane away from the center so that the degree of attenuation is varied. This needs calibration by a precise attenuator. To match the attenuator to the waveguide, the vane can be tapered at each end; usually a taper of $\lambda g/2$ provides an adequate match. Thus, it is frequency sensitive and the glass dielectric introduces appreciable phase shift.

Attenuation may also be obtained by inserting a resistive element through a shutter. The plane of the element lies in the distribution of the electric field across the wide dimension of the waveguide and the result is a degree of attenuation, which increases with the depth of insertion. However, due to the discontinuity, there is reflection of energy.

7.6. Movable-Vane (Flap) Attenuator

Figure 15 shows a waveguide variable, dissipative attenuator. The card enters the waveguide through the slot in the broad wall, thereby intercepting and absorbing a portion of the TE_{10} wave. The card penetration, and hence the attenuation, is controlled by means of the hinge arrangement to obtain variable attenuation. The ratings are typically 30 dB and are widely used in microwave equipment. However, the attenuation is frequency sensitive and the phase of the output signal is a function of card penetration and hence attenuation. This may result in nulling when the attenuator is part of a bridge network. Since it is not simple to calculate the loss in dB, this type of attenuator has to be calibrated against a superior standard. To overcome these drawbacks, a rotary-vane attenuator is used.

7.7. Rotary-Vane Attenuator

The rotary-vane attenuator is a direct-reading precision attenuator that obeys a simple mathematical law, $A = -20 \log \cos^2 \theta = -40 \log \cos \theta$ dB. As such, it is frequency-independent, which is a very attractive criterion

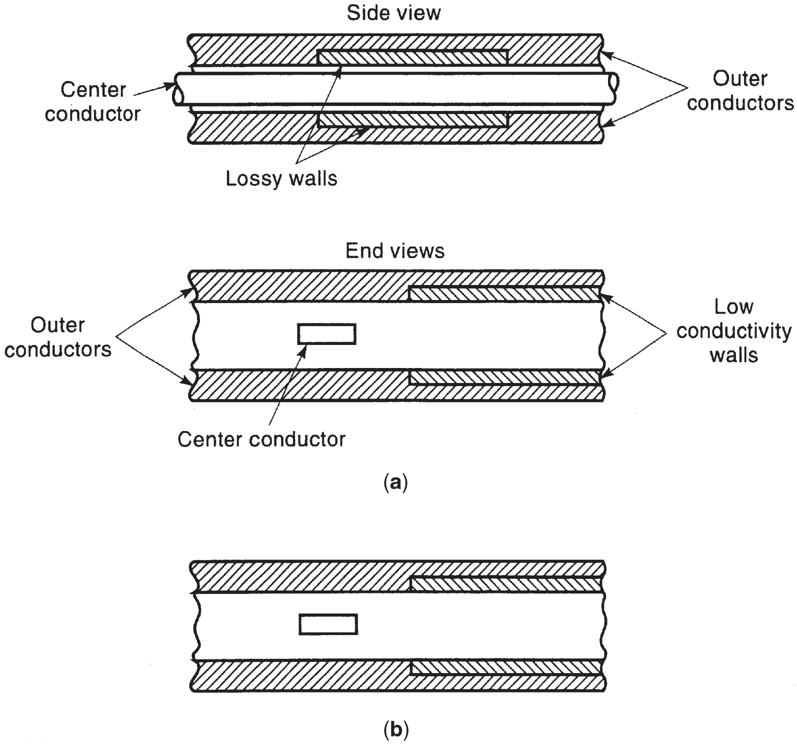

Figure 14. Lossy wall attenuator configuration: (a) minimum attenuator; (b) maximum attenuator.

for an attenuator. A functional diagram illustrates the operating principle of this attenuator. It consists of three sections of waveguide in tandem as shown (Fig. 16). A rectangular-to-circular waveguide transition containing a horizontal attenuator strip is connected to a rotatable circular waveguide containing an attenuator strip. This in turn is connected to a circular-to-rectangular waveguide transition containing a horizontal attenuator strip.

The incoming TE_{10} mode is transformed into the TE_{11} mode in the circular waveguide by the rectangular-to-circular waveguide transition with negligible reflections. The polarization of the TE_{11} mode is such that the e field is perpendicular to the thin resistive card in the transition section. As such, this resistive card has a negligible effect on the TE_{11} mode. Since the resistive card in the center can be rotated, its orientation relative to the electric field of the incoming TE_{11} mode can be varied so that the amount by which this mode is attenuated is adjustable.

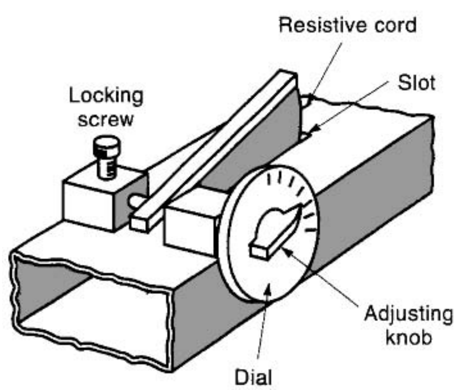

Figure 15. Movable-vane (flap) variable attenuator configuration.

When all the strips are aligned, the electric field of the applied wave is normal to the strips and hence no current flows in the attenuation strips and therefore no attenuation occurs. In a position where the central attenuation strip is rotated by an angle θ, the electric field of the applied wave can be resolved into two orthogonally polarized modes; one perpendicular and one parallel to the resistive card. That portion which is parallel to the resistive slab will be absorbed, whereas the portion, which is polarized perpendicular to the slab, will be transmitted.

7.8. Variable Coupler Attenuator

These are basically directional couplers where the attenuation is varied by mechanically changing the coupling between two sections. This is accomplished by varying the spacing between coupled lines. These attenuators have a large range, high power handling capability, and retain calibration over a range of ambient conditions. They have a higher insertion loss at lower frequencies (Fig. 17).

7.9. Absorptive Attenuator

Figure 18 shows an absorptive variable attenuator. Attenuation is obtained by using a lossy dielectric material. The TEM electric field is concentrated in the vicinity of the center strip of the stripline. When the absorbing material is inserted in the high-field region, a portion of the TEM wave is intercepted and absorbed by the lossy dielectric. Thus, the attenuation increases. Since the characteristic impedance of the stripline changes with the dielectric

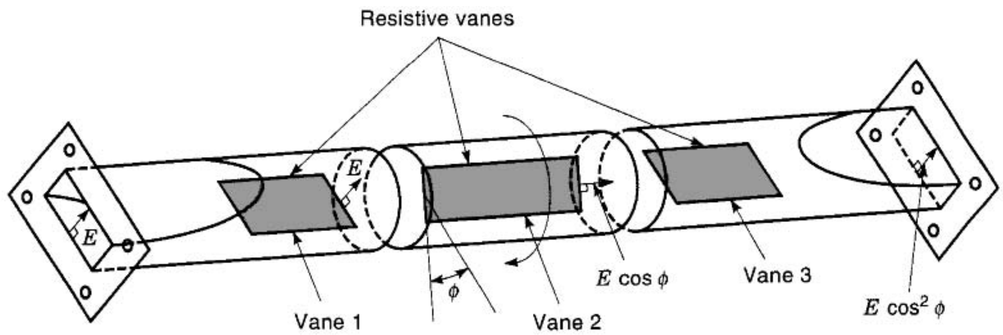

Figure 16. Rotary-vane attenuator configuration.

material insertion, the SWR tends to increase as the attenuation increases. To minimize this, the ends of the lossy material are tapered to provide a smooth impedance transformation into and out of the lossy section. SWR values of >1.5 are possible over a limited frequency range. In general, the SWR deteriorates at low frequencies. The attenuation increases with increasing frequency for a fixed setting. This is another disadvantage, since this makes the calibration a cumbersome procedure. Compensation techniques are occasionally used to reduce this variation with frequency.

7.10. Coaxial Resistive Film Attenuator

Figure 19 shows a coaxial resistive film attenuator. In this configuration, if r is the RF resistance per unit length, by adjusting the length l, the series resistance $R = rl$ of the center conductor is changed; thus, the attenuation is variable. If I is the conduction current on the center conductor, the voltage drop is $V = RI = Irl$. If E_i is the input voltage, then the output voltage is $E_0 = E_i - rlI$ and the attenuation is

$$A = 20 \log \frac{E_i}{E_i - rlI} (\text{dB}) \tag{35}$$

7.11. Variable T

The variable T attenuator is the same as the fixed attenuator except that the resistors are variable (Fig. 20). All three resistors are variable simultaneously to give good input/output VSWR.

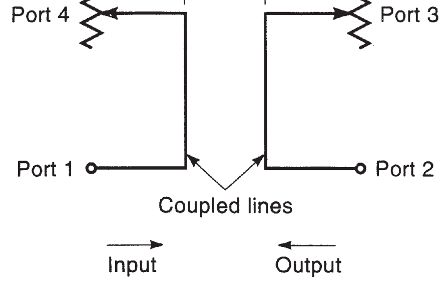

Figure 17. Variable coupler attenuator configuration.

7.12. Waveguide below Cutoff or Piston Attenuator

The simple principle of cutoff below frequency is used in the piston or the cutoff attenuator. The cylindrical waveguide used is operating at a frequency below cutoff. For high-power applications, a coaxial configuration is used. A simple waveguide cutoff attenuator is shown in Fig. 21. A metal tube, acting as a waveguide, has loops arranged at each end to couple from the coaxial lines into and out of the waveguide. One of the loops is mounted on a movable plunger or hollow piston so that the distance between the loops is variable. The input coupling loop converts the incoming TEM wave into the TE_{11} mode in the circular guide, while the output loop converts the attenuated TE_{11} mode back to TEM. The attenuator can be matched by adding Z_0 resistors. The attenuation is given as

$$A(\text{dB}) = 54.6 \frac{l}{\lambda_c} \sqrt{1 - \left(\frac{f}{f_c}\right)^2} \tag{36}$$

By choosing the diameter such that $\lambda_c \ll \lambda_o$, and hence $f/fc \ll 1$, this equation reduces to

$$A(\text{dB}) = 54.6 \frac{1}{\lambda_c} \tag{37}$$

This was obtained from

$$\alpha = \frac{2\pi}{\lambda_{oc}} \text{Np/m or } \alpha = \frac{54.6}{\lambda_{oc}} \text{dB/m where } 1\,\text{Np} = 8.686\,\text{dB} \tag{38}$$

[If $\lambda_{oc} = 10$ cm, and λ_o is much greater (10 times or more—in this case, 1 m or more), the attenuation

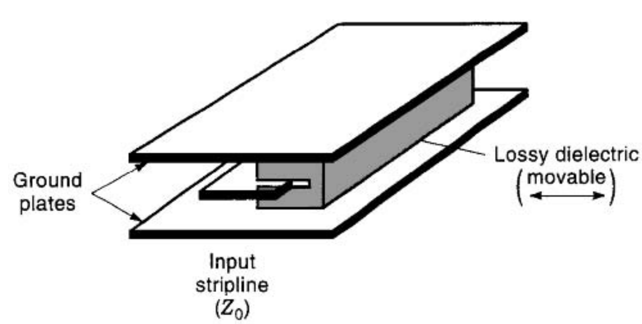

Figure 18. Absorptive-type variable attenuator configuration.

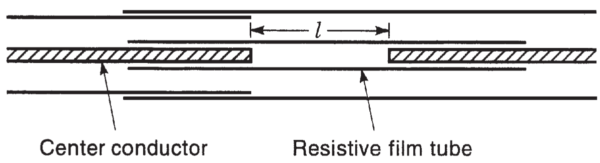

Figure 19. Coaxial resistive film attenuator configuration.

increases 5.45 dB per cm of outward movement of the plunger.]

The sliding cylindrical conductors allow length l to be varied, which varies the attenuation, since attenuation $A = \alpha l$, where α is the attenuation constant due to the cutoff effect, and l is the length of the circular guide. The cutoff wavelength is $\lambda_c = 1.706D$, where D is the diameter of the waveguide. Thus the attenuation is

$$A(\mathrm{dB}) = 54.6\,\frac{l}{\lambda_c} = 32\,\frac{l}{D} \tag{39}$$

or

$$\Delta A(\mathrm{dB}) = \frac{32}{D}\,\Delta l \tag{40}$$

The attenuation is independent of frequency; it depends only on the physical dimensions and hence can be accurately controlled by maintaining tight tolerances on the length and diameter of the circular guide. With ΔA linearly proportional to Δl, the cutoff attenuator is easily calibrated and hence particularly useful as a precision variable attenuator.

The cutoff attenuator is one of the most widely used precision variable attenuators in coaxial measurement equipment. This is a reflective-type attenuator, since the waveguide is essentially dissipationless. The signal is reflected rather than absorbed. For higher attenuation (>10 dB), the SWR at both ports is very high (>30). This can cause problems in certain applications.

This type of attenuator is very useful, but has the disadvantage of high insertion loss. Due to the nature of cutoff, the insertion loss is high, up to 15–20 dB. If this loss is overcome, piston attenuators are one of the most accurate attenuators available. Values of 0.001 dB/10 dB of attenuation over a 60 dB range are common. A good input/output match is obtained using inductive loops within the waveguides. Excellent matching is obtained over the entire range of attenuation due to inductive loop coupling. Figure 22 shows a commercially available standard variable piston attenuator and the various calibration curves. It contains an accurately dimensioned tube acting

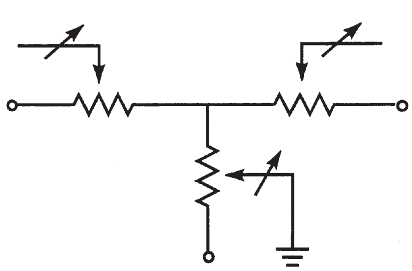

Figure 20. Variable T attenuator.

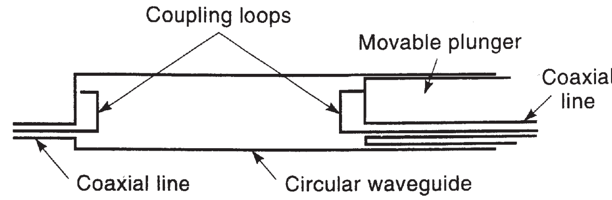

Figure 21. Coaxial variable cutoff attenuator configuration.

as a circular waveguide, below cutoff TE_{11} mode. Typical specifications are (courtesy of Weinschel Associates)

Frequency	30 MHz
Mode	TE_{11} cutoff
Range	0–120 dB 12.5 dB zero insertion loss
VSWR	1.2 max in 50-Ω system
Connectors	Type N, panel-mounted
Accuracy	0.01 dB from 0 to 15 dB 0.005 dB/10 dB from 15 to 100 dB 0.01 dB/10 dB from 100 to 120 dB
Resolution	0.001 dB direct-reading digital indicator

7.12.1. Laser Piston Attenuator. Figure 23 shows a laser piston attenuator. The heart of this instrument is a precise stainless steel circular waveguide, operated in the TE_{11} cutoff mode. Laser light, traveling between two antennas in the center of the circular waveguide, measures directly the changes in actual separation of the two antennas along the same path as the TE_{11} mode propagates. The laser signal is converted to attenuation in dB and corrected for skin effect, the refractive index of air, and changes relative to temperature of the waveguide and pressure. The specifications are (courtesy of Weinschel Associates)

Operating frequency	Dual frequency 1.25 MHz + 0.05 MHz and 30.0 MHz + 0.1 MHz
Waveguide mode	TE_{11}, below cutoff
Incremental attenuation range	100 dB
Minimum insertion loss	10 dB nominal
Resolution	0.0001 dB for Δ dB, 0.002 dB for total loss
Attenuation readout	Front panel 7-digit LED or remotely via IEEE bus
Connectors	Type N jacks
VSWR (input and output)	1.2 max at 1.25 and 30 MHz in 50-Ω system
Accuracy	0.001 dB/10 dB + 0.0005 dB between 15 and 115 dB total loss
Weight	Net: 77 kg (170 lb); shipping: 145 kg (320 lb)
Accessories	Power supply, controller, calibration tape, two power cables, one 22-wire power cable, instruction/maintenance manual

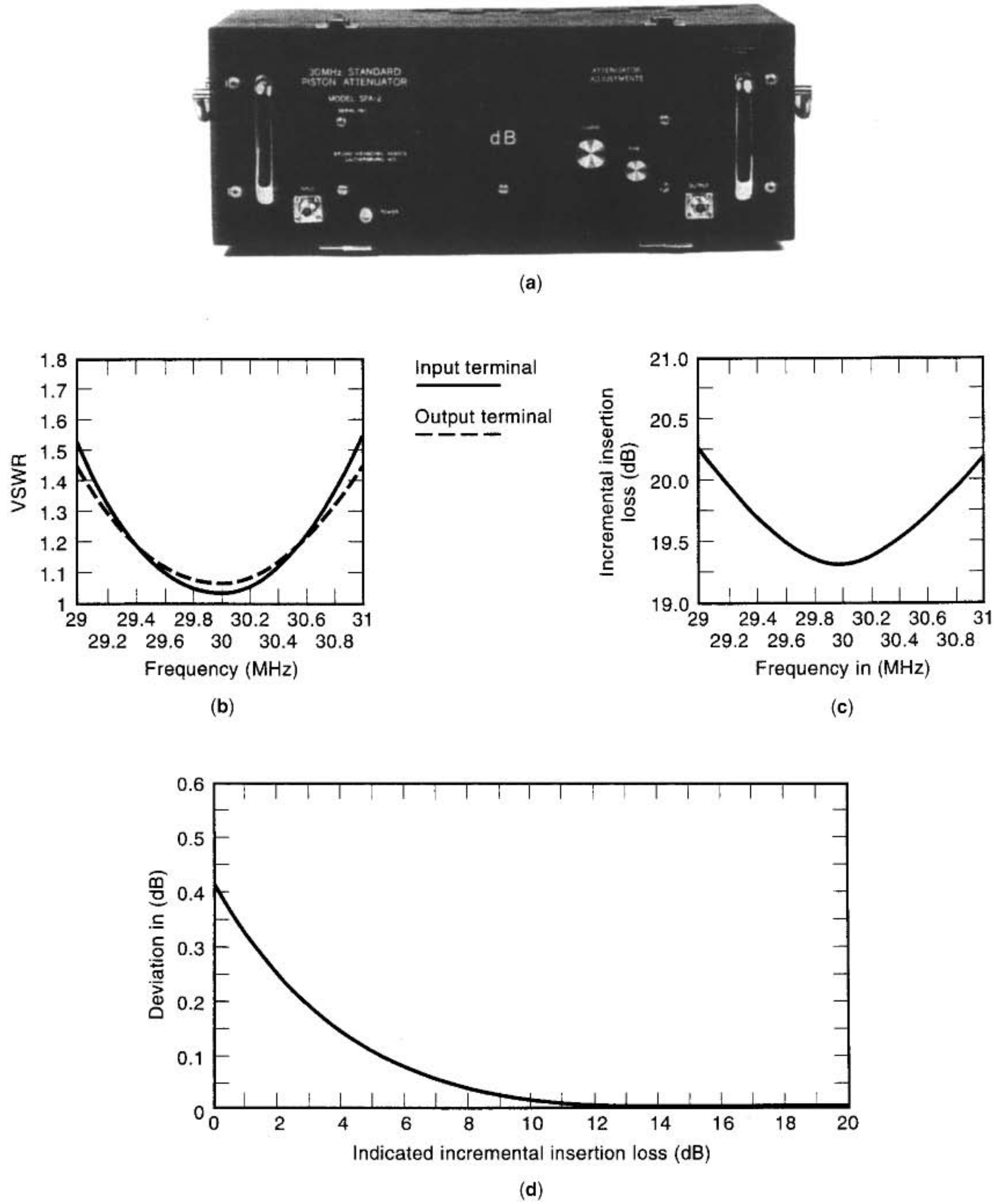

Figure 22. (a) Standard variable piston attenuator and (b–d) calibration curves. (b) Typical VSWR versus frequency of SPA-2 attenuator with frequency. (c) Typical variation of insertion loss of SPA-2 attenuator with frequency in a 50-Ω system. (d) Deviation versus indicated incremental insertion. Typical deviation from linearity for the model SPA-2 operating frequency is 30.0 MHz.

8. ACTIVE ATTENUATORS

8.1. pin Diode Attenuators

The normal diode junction consists of a p-type material brought together with an n-type material to form the familiar pn junction. The pin diode is distinguished from the normal pn junction type by an area called an *intrinsic region* sandwiched between the p^+-doped and n^+-doped silicon layers. This intrinsic layer has almost no doping and thus has a very large resistance. When a variable DC control voltage forward-biases the pin diode, the DC bias or control current causes it to behave as almost a pure resistance at RF frequencies, with a resistance value that can be varied over a range from 1 Ω to 10 kΩ. As the bias current is increased, the diode resistance decreases. This relation makes the pin diode ideally suited as a variable

Figure 23. Laser piston attenuator. (Courtesy of Weinschel Associates.)

attenuator for leveling and amplitude modulating a RF signal.

These attenuators provide local oscillator, IF, and RF signal level control throughout communications, measurement, and control circuits. One example is the reduction in the output of a receive mixer in a code-division multiple-access (CDMA) base station prior to the IF amplifier. Also, to provide one step of transmit level control with little degradation of the noise figure (NF), it could be used in a CDMA handset transmit chain between the mixer (upconverter) and the bandpass filter (Fig. 24). Since the attenuator is purely passive, it produces no additive noise and the NF is essentially its insertion loss. Even in the attenuator mode, the effect on the noise figure would be minimal.

In personal communication service (PCS) systems, the base stations may be fed from multiple picocells that are physically separated from it by up to 100 ft or more of coaxial cable. The signal levels coming into the base station will vary depending on the cable length and individual transponder power. It is desirable to keep the signals at uniform levels coming into the base station; to do so, it may be necessary to attenuate the stronger signals. An attenuator can be easily inserted for this purpose.

The upper end of a receiver's linear dynamic range is determined by the largest signal it can handle without being overdriven and producing unacceptable levels of distortion caused by device nonlinearities. Inserting an attenuator before a low-noise amplifier (LNA) in the presence of strong, in-band signals produces better reception by preventing them from overdriving the receiver's front end. This effectively shifts the dynamic range upward by the amount of attenuation. It must be remembered that when inserted into the system, the attenuator will also present a load and a source impedance to the previous and succeeding stages, respectively, hence the importance of the attenuator impedance match.

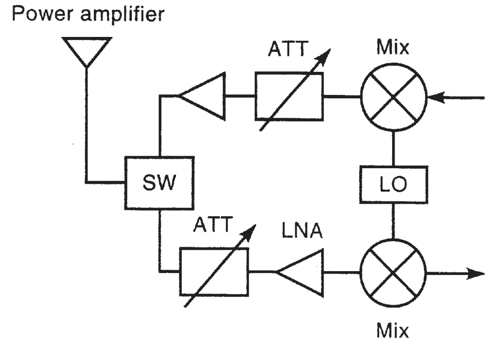

Figure 25. Functional block diagram of a digital cellular phone, using variable attenuators.

RF variable attenuators are used to control the transmitting and receiving signal power levels to prevent strong–weak adjacent signals from seriously degrading the bit error rate (BER) of digital mobile communication systems, such as TDMA or CDMA. Figure 25 shows the basic RF functional block diagram of a typical digital cellular phone system, where variable attenuators are required.

8.2. Characteristics of the pin Diode

The approximate high frequency equivalent circuit of a pin diode is shown in Fig. 26. Here, R_I is the effective resistance of the intrinsic (I) layer, given by

$$R_I = \frac{k}{I_{\mathrm{DC}}^x} \tag{41}$$

where I_{DC} is the DC bias current in mA, and k and x are device-dependent empirical constants. Although shown as a variable, this resistance is constant with respect to the RF signal. The high-frequency resistance function is plotted in Fig. 27 for the Hewlett-Packard HPND-4165 diode. For a specific diode design, the exponent X is usually a constant. For the HPND-4165, X is typically 0.92. The constant k and therefore R_I, however, are highly dependent on the fabrication and process control and its value can vary by as much as 3:1 from diode to diode. For analog applications, such as a variable attenuator, where repeatable attenuation with bias current is desired, the variation of R_I must be controlled. The HPND-4165 is

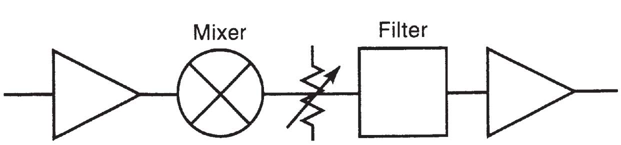

Figure 24. CDMA handset transmit application.

Figure 26. pin diode high-frequency equivalent circuit.

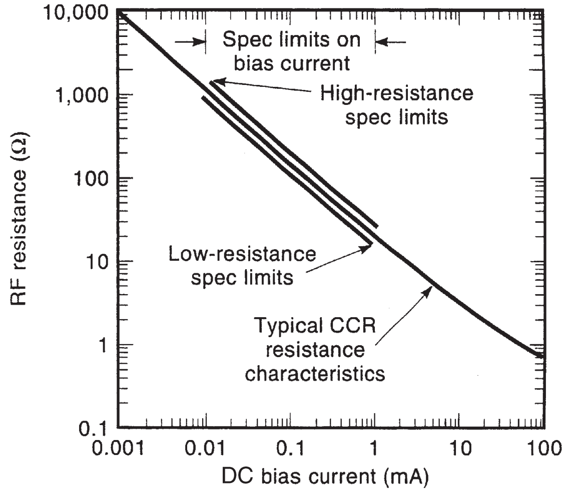

Figure 27. Typical RF resistance versus DC bias current for HPND-4165.

precisely controlled in manufacturing, and resistance values at specific bias points are specified and the slope of resistance versus bias matched with narrow limits. The specification limits of these parameters are shown in Table 4.

8.3. Applications

The pin diode is ideally suited to switch and attenuate RF signals. Since the pin diode is a RF variable resistor, the logical application is that of a variable attenuator. This attenuator may be either a step or a continuously variable type. Two of the simplest circuits are the series and shunt attenuators shown in Figs. 28 and 29.

Attenuation in the series pin circuit is decreased (more power appears at the output) as the RF resistance of the diode is reduced. This resistance is reduced by increasing the forward bias control current on the diode. The opposite occurs for the shunt configuration. The attenuation in the shunt circuit is decreased when the RF resistance of the diode increases because less power is absorbed in the diode and more appears at the output. If the control bias is switched rapidly between high and low (zero) values, then the circuit acts simply as a switch. When used as a switch, the attenuation that exists when the switch is ON is called

Table 4. HPND-4165 pin Diode Specifications

Parameter	HPND-4165	Test Conditions
High-resistance limit, R_H	1100–1660 Ω	10 μA
Low-resistance limit R_L	16–24 Ω	1 mA
Maximum difference in resistance versus bias slope x	0.04	10 μA and 1 mA

insertion loss. The attenuation provided when the switch is OFF is called *isolation*. If the diode is a pure resistance, the attenuation for the series and shunt circuit can be calculated as

$$A(\text{series}) = 20\ \log\left(1 + \frac{R_I}{Z_0}\right) \tag{42}$$

$$A(\text{shunt}) = 20\ \log\left(1 + \frac{Z_0}{2R_I}\right) \tag{43}$$

where $Z_0 = R_G = R_L =$ circuit, generator, and load resistance, respectively. In reviewing these equations, it is seen that the attenuation is not a function of frequency but only a ratio of circuit and diode resistances, which is a great advantage. As the bias on the diode is varied, the load resistance experienced by the source also varies. These circuits are generally referred to as reflective attenuators because they operate on the principle of reflection.

Many RF systems require that the impedance at both RF ports remain essentially constant at the design value Z_0. Four such circuits and their pin diode counterparts are shown in Fig. 30. All four circuits operate on the principle of absorbing the undesired RF signal power in the pin diodes. In circuits (a), (b), and (c), the control current variation through each diode is arranged in such a way that the impedance at both RF ports remain essentially constant at the characteristic impedance (Z_0) of the system while the attenuation can be varied over a range of less than 1 dB to greater than 20 dB. In circuit (d), the input impedance is kept constant by using a distributed structure with a large number of diodes. The impedance variation of each diode is also shaped so that the diodes in the center of the structure vary more than those near the ports. The resulting tapered impedance

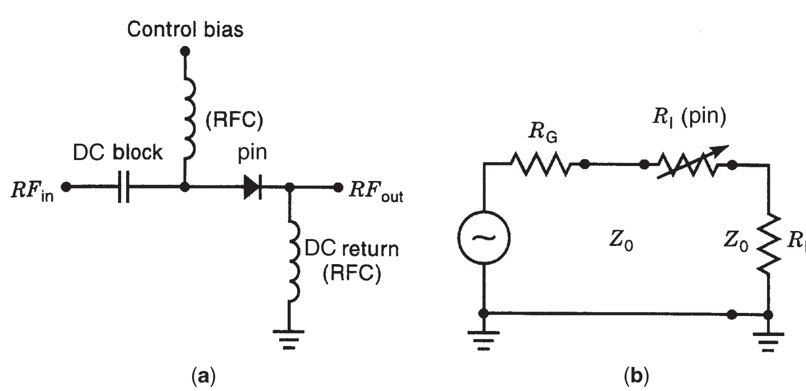

Figure 28. Series pin RF attenuator or switch: (a) complete circuit; (b) idealized RF equivalent circuit.

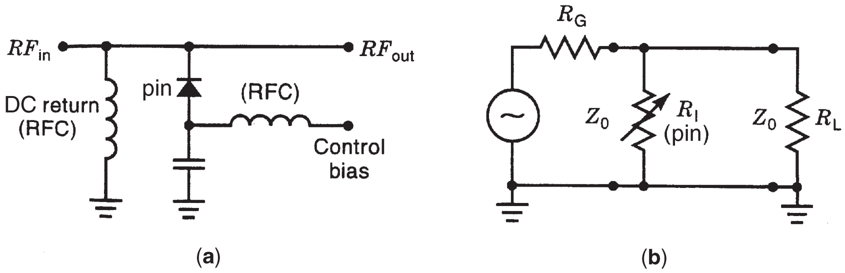

Figure 29. Shunt pin RF attenuator or switch: (a) complete circuit; (b) idealized RF equivalent circuit.

structure results in an essentially constant impedance at the ports, while the overall attenuation can be varied up to a range of 40–80 dB, depending on the length of the structure.

A pin diode pi attenuator such as that in Fig. 30a is often selected when designing a variable attenuator. The basic pi fixed attenuator is shown, along with its design equations, in Fig. 31. Shunt resistors R_1 and the series resistor R_3 are set to achieve a desired value of attenuation, while simultaneously providing an input and output impedance that matches the characteristic impedance Z_0 of the system.

Three pin diodes can be used as shown in Fig. 32 to replace the fixed resistors of the pi circuit to create a variable attenuator. The attenuator provides good performance over the frequency range of 10 MHz to over

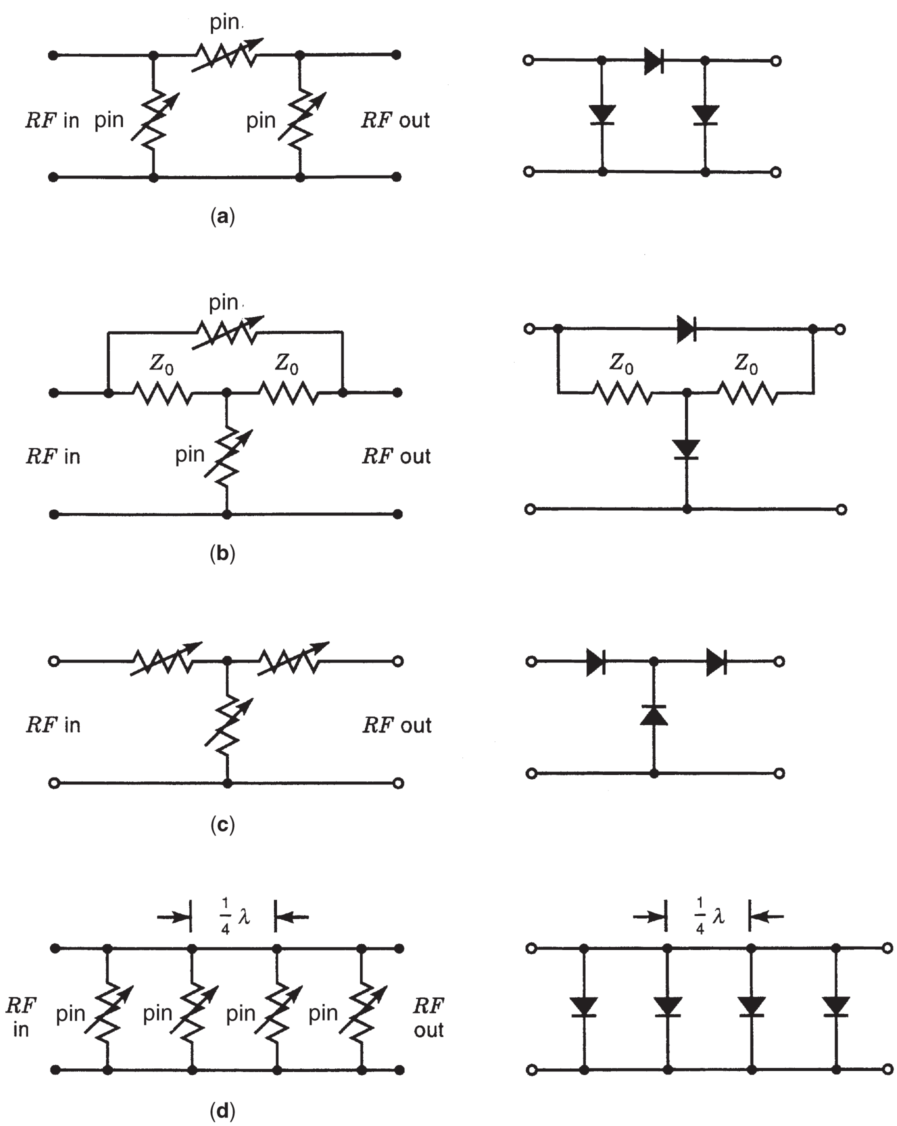

Figure 30. Constant impedance pin diode attenuators: (a) pi attenuator; (b) bridged T attenuator; (c) T attenuator; (d) resistive line attenuator.

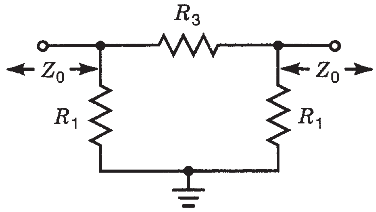

Figure 31. Fixed pi attenuator.

500 MHz. However, the use of three diodes as the three variable resistors in a pi attenuator results in a complex unsymmetric bias network. If resistor R_3 is replaced by two diodes, as shown in Fig. 33, the resulting attenuator is symmetric and the bias network is significantly simplified. V_+ is a fixed voltage, and V_c is the variable control voltage, which controls the attenuation of the network. The only drawback to using two series diodes in place of one is the slight increase in insertion loss. Resistors R_1 and R_2 serve as bias returns for series diodes D_2 and D_3. Resistors R_3 and R_4 are chosen to match the specific characteristics of the pin diodes used. Properly selected, they will provide the correct split of bias current between series and shunt diodes required to maintain a good impedance match over the entire dynamic range of attenuation.

The pin diode variable attenuator is an excellent circuit used to set the power level of an RF signal from a voltage control; it is used widely in commercial applications, such as cellular phones, PCN (personal communication networks), wireless LANs (local-area networks), and portable radios.

8.4. GaAs NMESFET Attenuator

The GaAs N-semiconductor metal semiconductor field effect transistor (NMESFET) is used in microwave attenuator designs. The metal–semiconductor FET (MESFET) is a field-effect transistor that operates on the principle that the gate-to-source voltage controls the drain current. The MESFET is a device extension of a JFET, where the gate structure is a Schottky MN (metal–N semiconductor) junction.

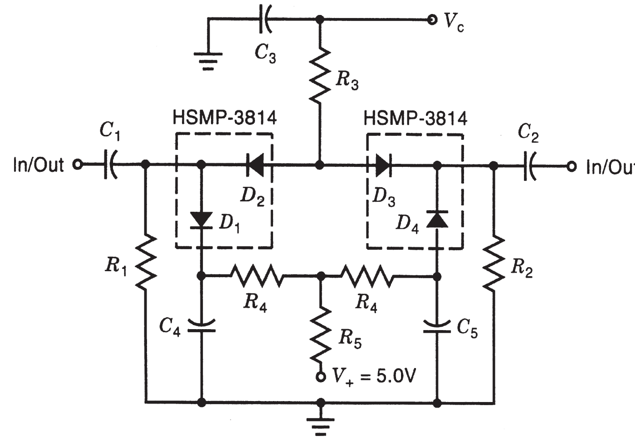

Component	Value	Manufacturer and part number
R_1, R_2	560 Ω	Kyocera CR21-561JB1
R_3	330 Ω	Kyocera CR21-331JB1
R_4	1640 Ω	Kyocera CR21-162JB1
R_5	680 Ω	Kyocera CR21-6B1JB1
C_1–C_5	47,000 pF	Kyocera 08957473M2P03
D_1–D_4	–	Hewlett-Packard HSMP-3814

Figure 33. Wideband four-diode II attenuator.

In GaAs NMESFET attenuator designs, the devices are operated either in the linear region where the device is modeled as a voltage variable resistor or as an ON/OFF switch in conjunction with thin-film nichrome resistors to provide appropriate levels of attenuation. The channel resistance of the GaAs NMESFET is known to follow the classical theory for a FET in the linear region of operation. With the FET biased in the linear region, the resistance varies inversely to the gate voltage as shown below:

$$R_{ds} = R_{ds0}\left(\frac{1}{1-(V_g/V_p)}\right) \tag{44}$$

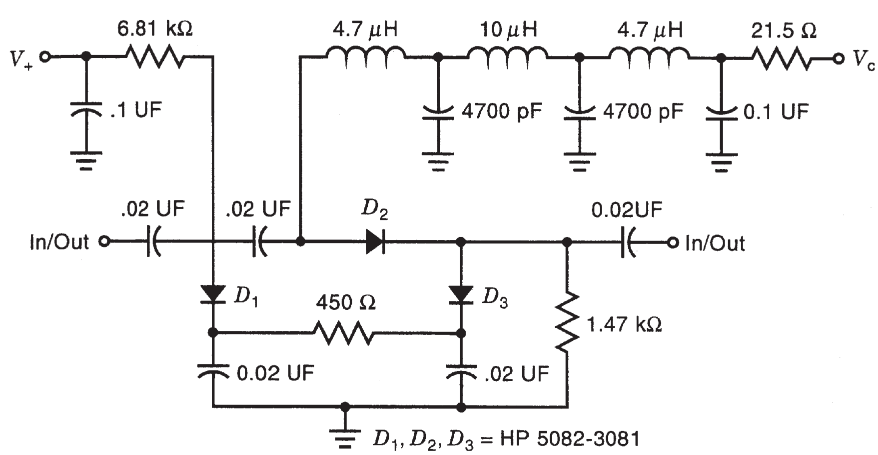

Figure 32. Three-diode pi attenuator.

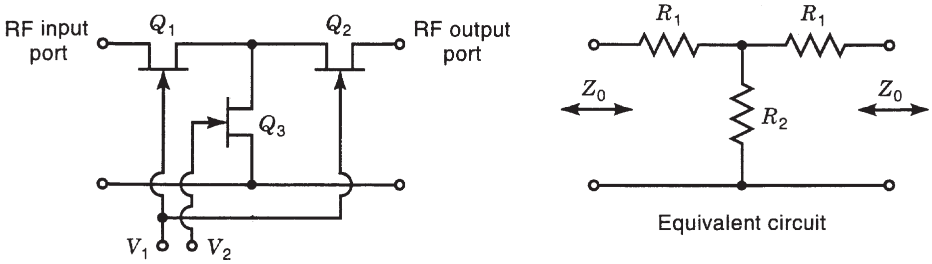

Figure 34. MESFET T attenuator.

where V_g = gate bias voltage (V), V_p = pinchoff voltage (V), and R_{ds0} = channel resistance (Ω) with $V_g = 0$ V.

As the gate voltage approaches the pinchoff voltage, the resistance becomes very high (relative to 50 Ω). Conversely, as the gate voltage approaches zero, so does the channel resistance. For each attenuator configuration, two independent gate bias voltages are used; one to control the series MESFETs and one to control the shunt MESFETs. The T attenuator configuration is shown in Fig. 34, with one voltage controlling the series resistance arms, and another the shunt resistance arm. Table 5 gives the resistor values of the series and shunt resistances in a $Z_0 = 50\,\Omega$ system. The channel resistances of the MESFETs are matched as closely as possible for these resistances. A matched condition at the input and output port to Z_0 occurs when

$$Z_0^2 = R_1^2 + 2R_1R_2 \tag{45}$$

The resulting matched attenuation is

$$A = 20\log\left(\frac{R_1 + R_2 + Z_0}{R_2}\right) \tag{46}$$

The pi attenuator configuration is shown in Fig. 35, with one voltage controlling the shunt resistance arms, and another the series resistance arm. Table 6 gives the values of the series and shunt resistances for different levels of attenuation in a $Z_0 = 50\,\Omega$ system. Shunt resistor R_1 and series resistor R_2 provide an input and output impedance that matches the characteristic impedance $Z_0 = 50\,\Omega$ of the system, while setting the desired level of attenuation. The design equations are

$$R_1 = Z_0\left[\frac{K+1}{K-1}\right] \tag{47}$$

$$R_2 = \frac{Z_0}{2}\left[K - \frac{1}{K}\right] \tag{48}$$

$$A(\mathrm{dB}) = 20\log K \tag{49}$$

where K is the input to output voltage ratio.

GaAs NMESFET digital attenuators allow a specific value of attenuation to be selected via a digital n bit programming word. In these designs, the NMESFET operates as an ON/OFF switch and is used in conjunction with nichrome thin-film resistors to provide the desired level of attenuation. Figure 36 shows the circuit configurations used for individual attenuator bits. The switched bridged T attenuator consists of the classical bridged T attenuator with a shunt and series FET. These two FETs are switched on or off to switch between the two states. The attenuation in dB is given by

$$A(dB) = 20\log\left(\frac{Z_0 + R_2}{R_2}\right) \tag{50}$$

where $Z_0^2 = R_1R_2$.

The performance is determined by the FET characteristics in the on and off states and the realizability limit on required resistance values and their associated parasitics. The switched T or pi attenuators are similar in principle to the switched bridged T attenuator except for the circuit topology. These attenuators are normally used for high attenuation values. To obtain smaller values of attenuation, the thin-film resistors are replaced with appropriate channel resistances.

There are GaAs NMESFET digital RF attenuators on the market with excellent performance, in both step and continuously variable types. The variable or programmable class allows a specific value of attenuation to be selected from an overall range via an N-bit programming word. They are more flexible than step attenuators, as they allow any amount of attenuation to be set, but the cost is greater circuit complexity. Both types have a bypass state when no attenuation is selected, and the attenuation is just the insertion loss of the device. An example of each type is presented.

Table 5. T Attenuator Resistor Values for Different Levels of Attenuation

Attenuation (dB)	R_1 (Ω)	R_2 (Ω)
2	5.73	215.24
4	11.31	104.83
6	16.61	66.93
8	21.53	47.31
10	25.97	35.14
12	29.92	26.81
14	33.37	20.78
22	42.64	7.99

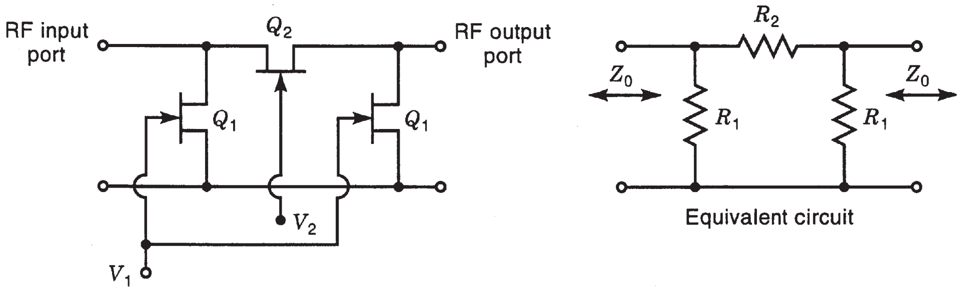

Figure 35. MESFET pi attenuator.

The RF Microdevices RF 2420 is a multistage monolithic variable or programmable attenuator that has as attenuation programmability over a 44 dB range in 2-dB steps. The attenuation is set by 5 bits of digital data. A functional block diagram of the RF 2420 is shown in Fig. 37. It consists of five cascaded, DC-coupled attenuator sections, each with its own logic translator. The logic translator converts the one-bit control signal, which uses logic levels approximating standard TTL logic, to the voltage levels required to switch the attenuator stage FETS. The RF input and output signal lines are biased at approximately V_{DD}, and therefore external DC blocking capacitors are required. An external V_{DD} bypass capacitor is also required.

A functional schematic of the RF portion of one attenuator section is shown in Fig. 38. A MESFET bridges the series resistor in a resistive pi attenuator, and two more MESFETs are connected as a double-pole single-throw (DPST) RF switch connecting the shunt branches of the pi attenuator to RF ground. In the bypass state, the bridge MESFET is in its high conductance state, and the DPST switch is open, so that the pi-attenuator is effectively removed from the circuit. When the attenuator bit is selected, the bridge MESFET is put into its low conductance state or cutoff state and the shunt FETs are put into their on state, so that the pi attenuator is connected into the RF series path. This attenuator has only moderate variation across a broad band of operation from 100 to 950 MHz, as illustrated in Fig. 39.

Furthermore, the attenuation varies smoothly and consistently with attenuator switch settings. Other features of the device are single 3–6-V supply operation, and 4 dB insertion loss, and the input and output have a low-VSWR 50-Ω match. All these features make the RF 2420 an excellent component for communications systems that require RF transmit power control by digital means. Typical applications are in dual mode IS-54/55 compatible cellular transceivers and TETRA systems. Figure 40 shows the complete schematic details of the RF 2420 being employed in a typical RF/IF switching attenuator application.

The RF Microdevice RF 2421 is a GaAs MESFET-switched step attenuator. It has a single-step digitally controlled attenuation of 10 dB. A functional block diagram of the device is shown in Fig. 41. The supply voltage range required is 2.7 V to 6 V DC. The input and output of the device have a low-voltage standing-wave ratio (VSWR) 50-Ω match, and the RF output can drive up to +16 dBm. It has 1.0 dB of insertion loss over the specified 500 MHz–3 GHz operating frequency range. The resistors are nickel chromium (nichrome) and provide excellent temperature stability. The RF ports are reversible, which means that the input signal can be applied to either port. The attenuation control pin has an internal pulldown resistor that causes the attenuator to be turned off when it is not connected. Figure 42 illustrates the RF 2421 being used to set the RF signal level in a communications system.

Table 6. Pi Attenuator Resistor Values for Different Levels of Attenuation

Attenuation (dB)	R_1 (Ω)	R_2 (Ω)
2	436	11.61
4	221	23.85
6	150.5	37.35
8	116.14	52.84
10	96.25	71.15
12	83.54	93.25
14	74.93	120.31
22	58.63	312.90

8.5. MOSFET Attenuators

Active voltage attenuators have many useful applications in analog integrated circuit design. Some of the applications are in the feedback loops of finite gain amplifiers and in the input stages of transconductance amplifiers. In discrete circuit design, the most popular way to design a finite-gain amplifier with precisely controlled gain, high linearity, and low output noise is to use operational amplifier and a voltage attenuator in the feedback loop. Here the voltage attenuator consists of two resistors connected in series as shown in the classical noninverting and inverting op amp gain configurations of Fig. 43. Resistor attenuators are not useful in integrated circuit design because of their large areas, low input impedance, large power dissipation, and parasitic capacitances, and precise resistance values cannot be realized.

Three MOS active voltage attenuator configurations useful for the realization of finite-gain amplifiers in mono-

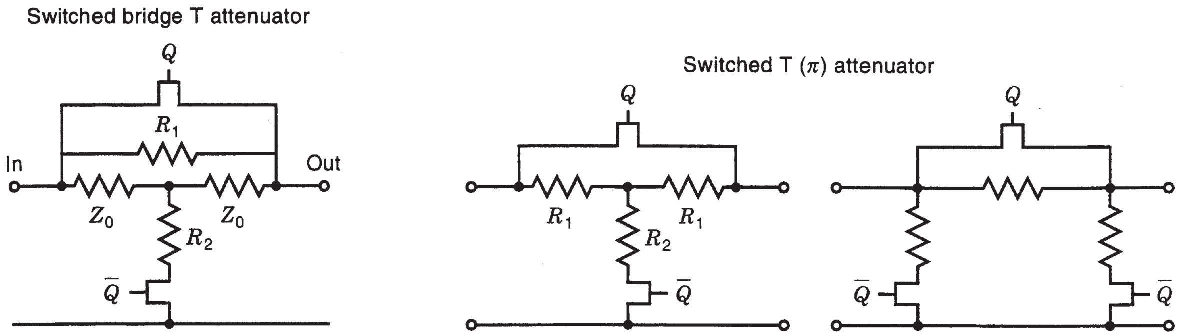

Figure 36. GaAs digital attenuator circuit configuration.

lithic circuits are presented. The attenuators are two single-input attenuators and a summing attenuator that has two inputs. These attenuators are simple in structure, consisting only of MOSFETs. Therefore, they are easy to fabricate in standard CMOS semiconductor processes. The attenuation factor is precisely controlled over a wide range of gains because it ideally depends only on the ratios of the dimensions of the MOSFETs.

Attenuator I, shown in Fig. 44, is an active linear voltage attenuator consisting of two n-channel MOSFETs fabricated in a common substrate. The capability to fabricate the MOSFETs in a common substrate has several advantages. First, both n-channel and p-channel attenuators can be monolithically fabricated in a standard CMOS process. Second, the required area of the attenuator is much smaller. As seen in Fig. 44, the substrate is common for both MOSFETs and is connected to the source of the bottom transistor M1. The circuit operates as a linear voltage attenuator when M1 is in the ohmic region and M2 is in the saturation region.

The operating conditions of the *MOS* attenuators in this section are derived as in the following equations,

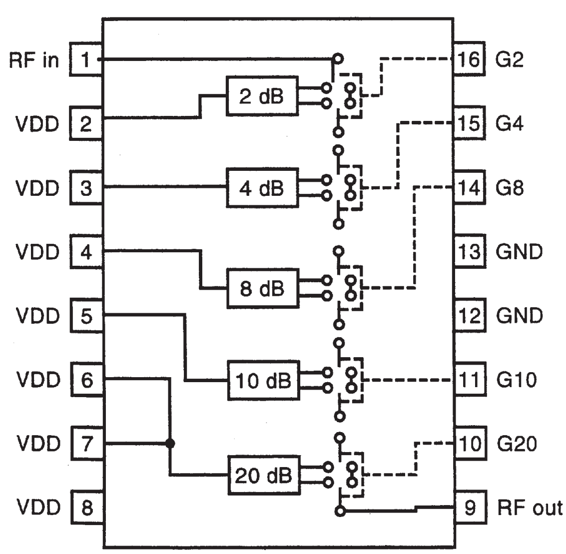

Figure 37. RF 2420 functional block diagram.

where

V_{in}	Input voltage
V_{out}	Output voltage
V_{DD}	Drain supply voltage
V_B	Bias supply voltage 1
V_{BB}	Bias supply voltage 2
$V_{TON} = V_{TON1} = V_{TON2}$	Zero bias threshold voltage of M1 and M2
V_{T2}	Threshold voltage of M2 due to body bias effect
V_1	Input voltage 1
V_2	Input voltage 2
γ	Body effect parameter
ϕ	Barrier potential
I_D	Drain current
W	Width of channel
L	Length of channel
W_1, W_2	Width of channels 1,2
L_1, L_2	Length of channels 1,2
K'	Device constant, μ_n CoX
μ_n	Mobility of electron
CoX	Gate oxide capacitance per unit area

The zero-bias threshold voltage of both MOSFETs is $V_{TON1} = V_{TON2} = V_{TON}$. The proper operating conditions will be met, provided

$$V_{TON} < V_{in} < V_{DD} + V_{T2} \tag{51}$$

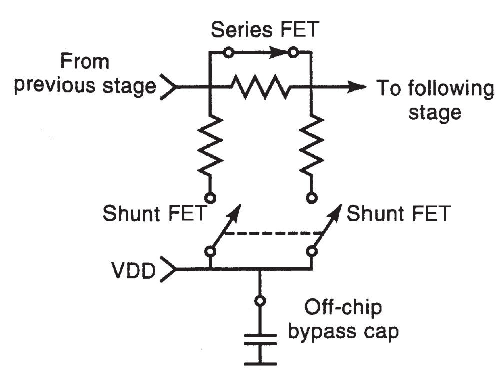

Figure 38. Functional schematic of RF 2420 (one attenuator section).

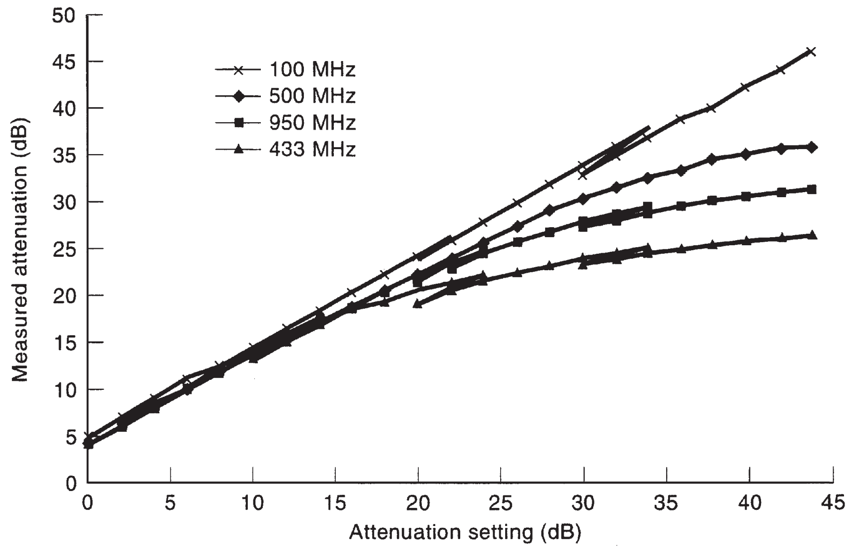

Figure 39. Attenuation and frequency response characteristics of RF 2420 5-bit digital RF attenuator.

where

$$V_{T2} = V_{TON} + \gamma\left(\sqrt{\phi + V_{out}} - \sqrt{\phi}\right) \qquad (52)$$

Since M1 is operating in the ohmic region and M2 is in the saturation region, the drain current of each MOSFET is given by

$$I_{D1} = K' \frac{W_1}{L_1}\left(V_1 - V_{TON} - \frac{V_{out}}{2}\right)V_{out} \qquad (53)$$

and

$$I_{D2} = K' \frac{W_2}{2L_2}(V_I - V_{T2} - V_{out})^2 \qquad (54)$$

Equating the two drain currents, the relationship between V_{in} and V_{out} is obtained as

$$2R\left(V_{in} - V_{TON} - \frac{V_{out}}{2}\right)V_{out} = \left\{V_{in} - V_{TON} - V_{out} - \gamma\left(\sqrt{\phi + V_{out}} - \sqrt{\phi}\right)\right\}^2 \qquad (55)$$

where

$$R = \frac{W_1/L_1}{W_2/L_2} \qquad (56)$$

If each MOSFET in the attenuator is fabricated in a separate substrate and the substrate of each

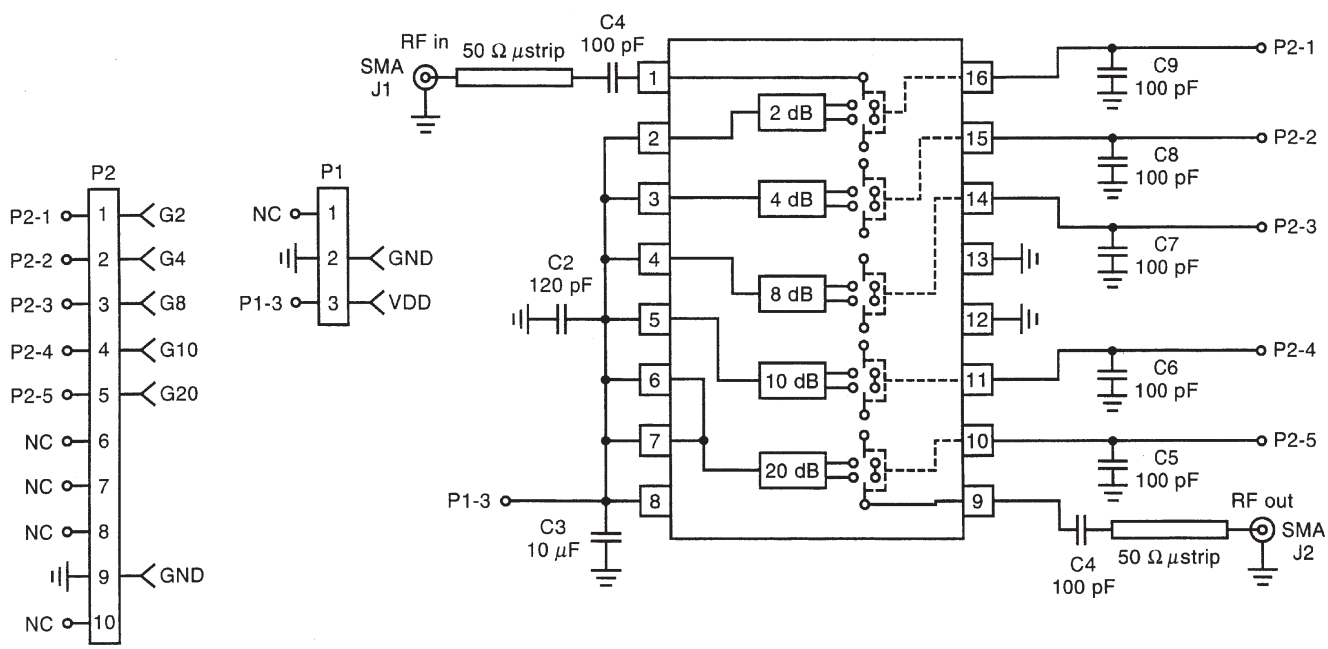

Figure 40. RF 2420 RF/IF switching attenuator schematic.

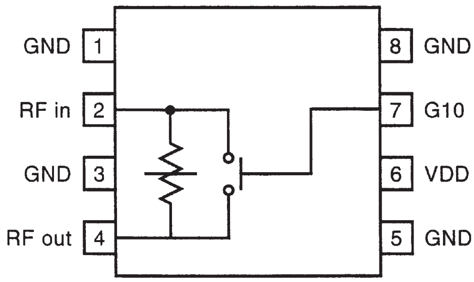

Figure 41. RF 2421 functional block diagram.

MOSFET is connected to its source ($\gamma = 0$), the DC transfer characteristic relating $V_{\rm in}$ and $V_{\rm out}$ becomes a linear equation:

$$V_{\rm out} = \alpha(V_{\rm in} - V_{\rm TON}) \tag{57}$$

where α is the small-signal attenuation factor.

In this case, α is

$$\alpha = 1 - \sqrt{\frac{R}{R+1}} = 1 - \sqrt{\frac{W_1/L_1}{W_1/L_1 + W_2/L_2}} \tag{58}$$

Equation (57) is a special case of Eq. (55), when the bulk effect term due to γ is ignored. When the substrate is separate, the small-signal attenuation factor from Eq. (58) is precisely determined by width/length ratios. If the substrate is common, the relationship between the input and output is still very linear as given by Eq. (55) even though the equation appears to be a nonlinear quadratic.

Figure 45 shows the typical DC transfer characteristic of the attenuator consisting of M1 ($12 \times 10\,\mu\text{m}^2$) and M2 ($3 \times 10\,\mu\text{m}^2$) when the substrate is common ($\gamma \neq 0$) and $V_{\rm DD} = 5$ V. The DC transfer characteristic exhibits a high degree of linearity for the input range 2–5 V. The small-signal attenuation factor (α), which is the slope of the DC transfer characteristic is 0.07824 at an input quiescent voltage of 3.5 V.

A finite-gain amplifier consisting of an ideal op amp and attenuator I in the feedback loop is shown in Fig. 44. Since the op amp is assumed ideal, we obtain

$$V_{\rm in} = V_{\rm out} = \alpha V_{\rm in} = \alpha V'_{\rm out} \tag{59}$$

or

$$V'_{\rm out} = \frac{1}{\alpha} V'_{\rm in} \tag{60}$$

Thus, the DC transfer function of the amplifier is the inverse function of the DC transfer function of the attenuator in the feedback loop. Thus, the transfer function between the input $V'_{\rm in}$ and the $V'_{\rm out}$ of the amplifier is given by Eq. (55) when $V_{\rm out}$ is replaced by $V'_{\rm in}$ and $V'_{\rm in}$ by $V'_{\rm out}$. The small-signal voltage gain

$$\left(A_V = \frac{V'_{\rm out}}{V'_{\rm in}} = \frac{1}{\alpha}\right)$$

is the reciprocal of the attenuator's attenuation factor in the feedback loop. Figure 46 illustrates the DC transfer characteristic of the finite-gain amplifier.

Two slightly different linear inverting voltage attenuator configurations consisting of two n-channel MOSFETs are shown in Fig. 47. These circuits operate as a linear inverting voltage attenuator when both transistors are in the saturation region. Assuming the zero-bias threshold of both of the MOSFETs is $V_{\rm TON}$, the condition will be met, provided

$$V_{\rm out} + V_{\rm T2} < V_{\rm B} < V_{\rm DD} + V_{\rm T2} \tag{61}$$

and

$$V_{\rm TON} < V_{\rm in} < V_{\rm out} + V_{\rm TON} \tag{62}$$

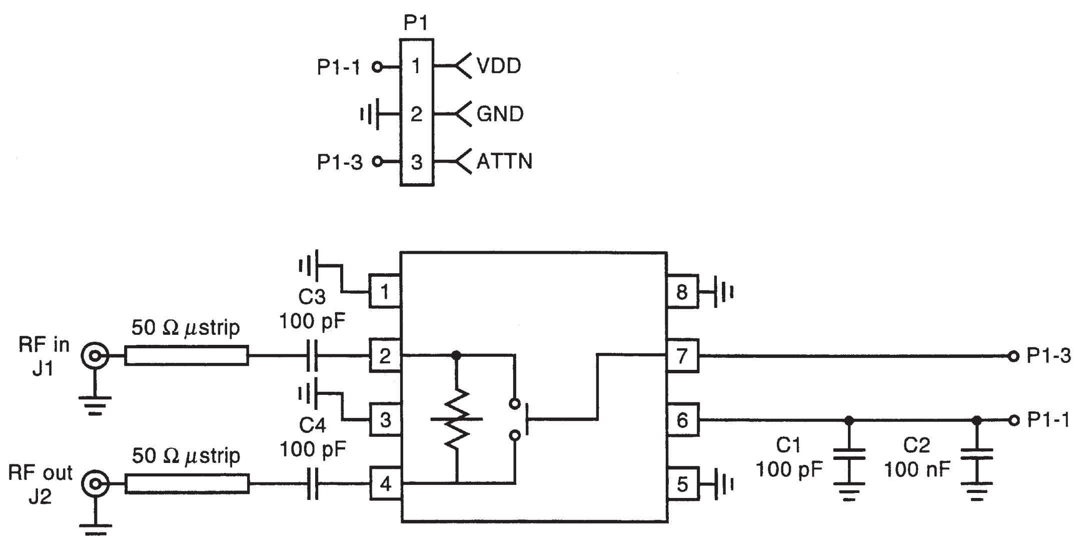

Figure 42. RF 2421 single-step 10-dB attenuator application.

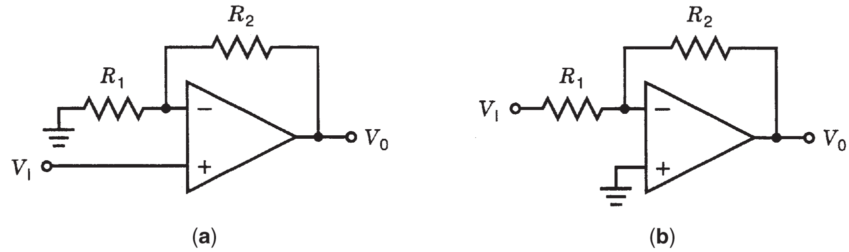

Figure 43. Op amp noninverting (a) and inverting (b) gain configuration.

Under this condition, the drain currents of the transistors are given by

$$I_{D1} = K' \frac{W_1}{2L_1}(V_{in} - V_{TON})^2 \tag{63}$$

$$I_{D2} = K' \frac{W_2}{2L_2}(V_B - V_{out} - V_{T2})^2 \tag{64}$$

where

$$V_{T2} = V_{TON} + \gamma(\sqrt{\phi + V_0} - \sqrt{\phi}) \tag{65}$$

Since the two drain currents are the same for the circuit, the DC transfer function relating V_{in} and V_{out} is found by equating Eqs. (63) and (64):

$$\begin{aligned} &V_{out} + \gamma\left(\sqrt{\phi + V_{out}} - \sqrt{\phi}\right) \\ &= -R_1 V_{in} + \{V_B + (R_1 - 1)V_{TON}\} \end{aligned} \tag{66}$$

where

$$R_1 = \sqrt{\frac{W_1/L_1}{W_2/L_2}} \tag{67}$$

If $\gamma = 0$ in Eq. (66), which corresponds to the case of circuit (b) in Fig. 47, where the substrate is separate, the DC transfer characteristic reduces to a linear equation:

$$V_{out} = \alpha V_I + \{V_B - (\alpha + 1)V_{TON}\} \tag{68}$$

In this case, the small-signal attenuator factor is

$$\alpha = -R_1 \tag{69}$$

which is precisely determined by the width/length ratios of the MOSFETs. From Eqs. (66) and (68), it is noted that the output DC operating voltage is controlled by V_B, independent of the attenuation factor.

The DC transfer characteristic between V_{in} and V_{out} calculated from Eq. (66) for the common substrate case, $R_1 = 0.1149$ and $V_B = 3.993$, and the DC transfer characteristics calculated from Eq. (68) for the separate substrate case, $R_1 = 0.1$ and $V_B = 3.449$ are shown in Fig. 50 for the range restricted by Eq. (62). The parameter values ($\gamma = 0.525\,V^{1/2}$, $\phi = 0.6\,V$, and $V_{TON1} = V_{TON2} = V_{TON} = 0.777\,V$) were used in the calculation. The DC transfer function given by Eq. (66) for the common substrate case appears nonlinear, but the degradation from linearity due to practical values of γ is not significant. The small-signal attenuation factor α, the slope of transfer characteristic in Fig. 48, is -0.1. The high degree of linearity supports the usefulness of both configurations in precision attenuator or finite-gain amplifier applications.

Figure 49 shows a finite-gain amplifier with attenuator II in the feedback loop of an op amp. Assuming that the op amp is ideal, we obtain

$$V'_{out} = \frac{1}{\alpha} V'_{in} \tag{70}$$

The transfer function of the amplifier is the inverse function of the transfer function of the attenuator in the feedback loop. The DC transfer function of the amplifier is given by Eq. (66) when V_{in} is replaced by V'_{out} and V_{out} is replaced by V'_{in}. If the substrate is separate, V_{in} replaces V'_{out} and V_{out} replaces V'_{in} in Eq. (68); then

$$V'_{out} = \frac{1}{\alpha} V'_I - \frac{1}{\alpha}\{V_B - (\alpha + 1)V_{TON}\} \tag{71}$$

where the small-signal attenuator factor $\alpha = -R_1$.

A summing attenuator is necessary to realize versatile multiple-input finite-gain amplifiers in integrated circuits. Figure 50 shows a two-input active linear inverting voltage summing attenuator that consists of two attenuators cascaded. For the summing attenuator, V_{BB} is used to control the output DC operating voltage, and input signals are designated as V_1 and V_2.

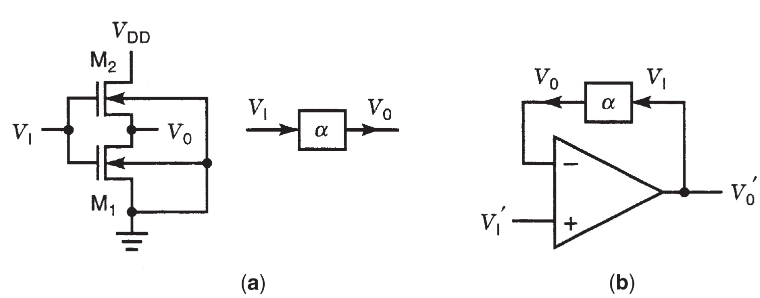

Figure 44. (a) Circuit and block diagram of attenuator I consisting of two n-channel MOSFETs, and (b) block diagram of amplifier consisting of an op amp and attenuator.

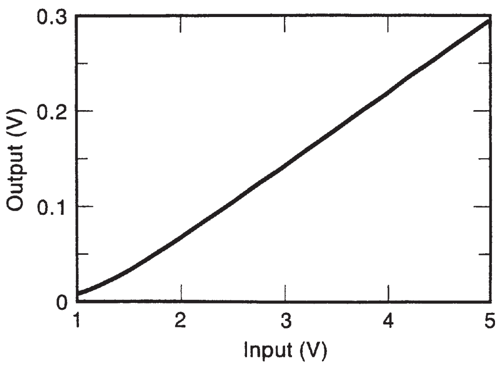

Figure 45. DC transfer characteristic of attenuator I ($\alpha = 0.07824$).

As for the inverting attenuator, the summing attenuator works when all the MOSFETs M1–M4 are operating in the saturation region. The DC transfer characteristics are found by equating the drain currents in the saturation region for each transistor. Assuming that the zero-bias threshold voltages for the four MOSFETs are matched at V_{TON}, the four transistors are in the saturation region, provided

$$2\left(V_{\mathrm{TON}} + \gamma\left(\sqrt{\phi + V_{\mathrm{TON}}} - \sqrt{\phi}\right)\right) + V_{\mathrm{out}} < V_{\mathrm{BB}} < V_{\mathrm{DD}} + V_{\mathrm{T4}} \tag{72}$$

$$V_{\mathrm{TON}} < V_1 < V_0 + V_{\mathrm{TON}} \tag{73}$$

$$V_{\mathrm{TON}} < V_2 < V_{\mathrm{B}} + V_{\mathrm{TON}} \tag{74}$$

By equating the drain currents of M3 and M4 given by

$$I_{\mathrm{D3}} = K' \frac{W_4}{2L_3}(V_2 - V_{\mathrm{TON}})^2 \tag{75}$$

and

$$I_{\mathrm{D4}} = K' \frac{W_4}{2L_4}(V_{\mathrm{BB}} - V_{\mathrm{B}} - V_{\mathrm{T4}})^2 \tag{76}$$

where

$$V_{\mathrm{T4}} = V_{\mathrm{TON}} + \gamma\left(\sqrt{\phi + V_0} - \sqrt{\phi}\right) \tag{77}$$

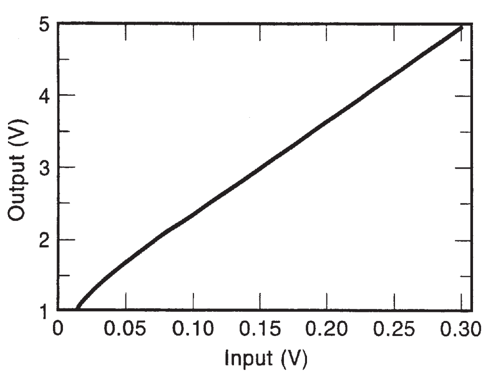

Figure 46. DC transfer characteristic of amplifier ($A_{\mathrm{V}} = 1/\alpha = 12.78$).

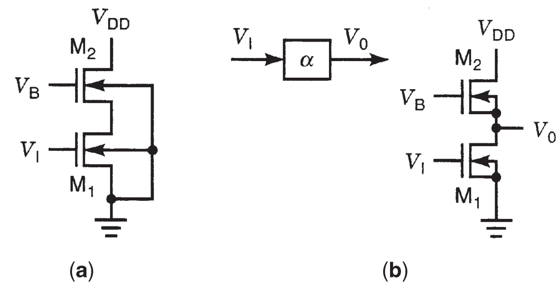

Figure 47. Circuit and block diagrams of linear inverting voltage attenuators consisting of two n-channel MOSFETs.

The DC transfer function between V_2 and V_{B} is obtained as

$$\begin{aligned} &V_{\mathrm{B}} + \gamma\left(\sqrt{\phi + V_{\mathrm{B}}} - \sqrt{\phi}\right) \\ &= -R_2 V_2 + \{V_{\mathrm{BB}} + (R_2 - 1)V_{\mathrm{TON}}\} \end{aligned} \tag{78}$$

where

$$R_2 = \sqrt{\frac{W_3 L_4}{L_3 W_4}} \tag{79}$$

Similarly, it can be shown that the DC transfer function between V_1 and V_0 is obtained as

$$\begin{aligned} &V_0 + \gamma(\sqrt{\phi + V_0} - \sqrt{\phi} \\ &= -R_1 V_1 + \{V_{\mathrm{B}} + (R_1 - 1)V_{\mathrm{TON}}\} \end{aligned} \tag{80}$$

where

$$R_1 = \sqrt{\frac{W_1 L_2}{L_1 W_2}} \tag{81}$$

If $\gamma = 0$ in Eqs. (78) and (80), the equations become linear. This is realized if each transistor is fabricated in a separate substrate and the substrate of each transistor is connected to its source. In this case, the attenuation

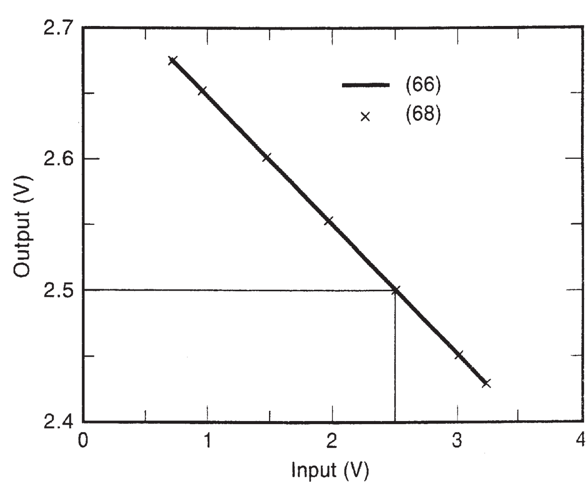

Figure 48. DC transfer characteristics of attenuator II linear inverting voltage attenuators.

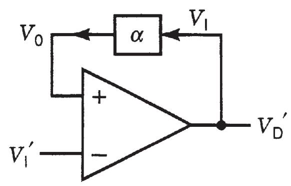

Figure 49. Amplifier consisting of op amp and attenuator II in the feedback loop.

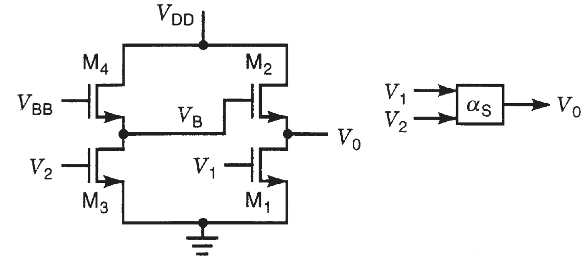

Figure 50. Circuit and block diagram of summing attenuator.

factors are given by $\alpha_1 = -R_1$, and $\alpha_2 = -R_2$. Even when $\gamma \neq 0$, which is the case when the substrates are common, the transfer characteristics between V_1 and V_0 and between V_2 and V_0 are nearly linear as shown in Fig. 53 for practical values of γ. In the calculation of Fig. 51, $\gamma = 0.5255\,\mathrm{V}^{1/2}$, $\phi = 0.6\,\mathrm{V}$, and $V_{\mathrm{TON}} = 0.777\,\mathrm{V}$ were used, which are standard for a 2μ CMOS process and $R_1 = 0.1149$ and $R_2 = 0.1290$ were set such that the small-signal attenuation factors for V_1 and V_2 are both -0.1. The operating points were set by $V_{\mathrm{BB}} = 5.712\,\mathrm{V}$ such that $V_{0\mathrm{Q}} = 2.5\,\mathrm{V}$ ($V_{\mathrm{BQ}} = 3.993\,\mathrm{V}$) when $V_{1\mathrm{Q}} = V_{2\mathrm{Q}} = 2.5\,\mathrm{V}$.

Summing and subtracting amplifier configurations using the inverting attenuator and the inverting summing attenuator are shown in Fig. 52.

Circuit (a) in Fig. 52 functions as a summing amplifier and the circuit (b) functions as a subtracting amplifier, with controllable weights. Assuming ideal op amps and attenuators, we obtain

$$V_- = \alpha_1 V_1 + \alpha_2 V_2 + \{V_{\mathrm{BB}} - (\alpha_1 + \alpha_2 + 2)V_{\mathrm{TON}}\} \tag{82}$$

$$V_+ = \alpha V_0 + \{V_{\mathrm{B}} - (\alpha + 1)V_{\mathrm{TON}}\} \tag{83}$$

Equating V_- and V_+, the output is given by

$$\begin{aligned} V_0 = {}& \frac{\alpha_1}{\alpha} V_1 + \frac{\alpha_2}{\alpha} V_2 + \frac{1}{\alpha} \\ & \{V_{\mathrm{BB}} - V_{\mathrm{B}} - (\alpha_1 + \alpha_2 - \alpha + 1)V_{\mathrm{TON}}\} \end{aligned} \tag{84}$$

From Eq. (84), the circuit in Fig. 52a is a summing amplifier with a wide range of available gain from each input. Similarly, for the circuit in Fig. 52b, we obtain

$$V_+ = \alpha_1 V_0 + \alpha_2 V_2 + \{V_{\mathrm{BB}} - (\alpha_1 + \alpha_2 + 2)V_{\mathrm{TON}}\} \tag{85}$$

$$V_- = \alpha V_1 + \{V_{\mathrm{B}} - (\alpha + 1)V_{\mathrm{TON}}\} \tag{86}$$

Equating V_+ and V_-, the output is given by

$$\begin{aligned} V_0 = {}& \frac{\alpha}{\alpha_1} V_1 - \frac{\alpha_2}{\alpha_1} V_2 - \frac{1}{\alpha_1} \\ & \{V_{\mathrm{BB}} - V_{\mathrm{B}} - (\alpha_1 + \alpha_2 - \alpha + 1)V_{\mathrm{TON}}\} \end{aligned} \tag{87}$$

From Eq. (87), the circuit in Fig. 52b is a subtracting amplifier with a wide range of available gain for each input.

The active attenuator and the active summing attenuator have many desirable characteristics such as small size, nearly infinite impedance, low power dissipation, and precisely controllable attenuation ratio with excellent linearity. These attenuators and the finite-gain amplifiers obtained from these attenuators and op amps will find increased applications in analog integrated circuits.

8.6. Noise

Noise in a communication system can be classified in two broad categories, depending on its source. Noise generated by components within a communication system, such as resistive, extender, and solid-state active devices, comprise internal noise. The second category, external noise, results from sources outside a communication system, including atmospheric, manmade, and extraterrestrial sources.

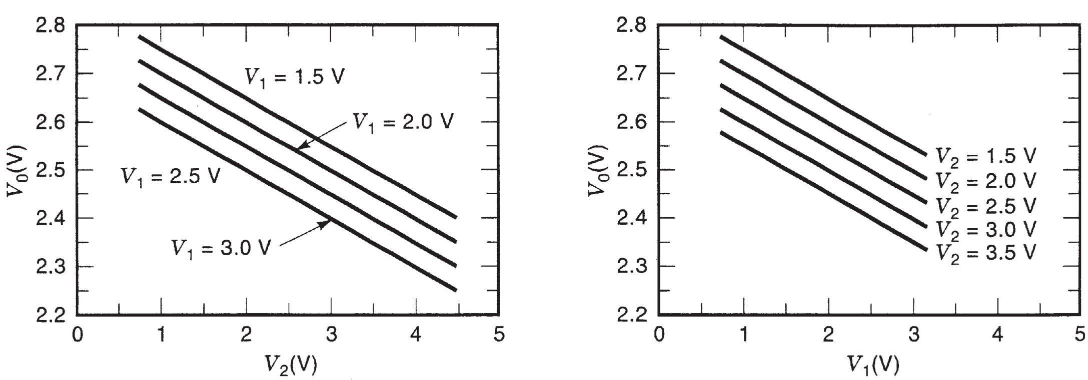

Figure 51. DC transfer characteristics of summing attenuator.

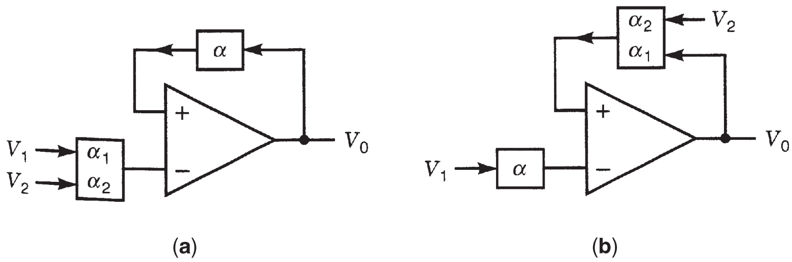

Figure 52. (a) Summing amplifier; (b) subtracting amplifier.

External noise results from the random motion of a charge carrier in electronic components. The three types are

1. Thermal noise: caused by random motion of free electrons in a conductor or semiconductor excited by thermal agitation
2. Shot noise: caused by random amount of discrete charge carriers in such devices as thermionic tubes or semiconductors in devices
3. Flicker noise: produced by semiconductors by a mechanism not well understood and is more severe the lower the frequency

Atmospheric noise results primarily from spurious radiowaves generated by the natural discharges within the atmosphere associated with thunderstorms. Manmade noise sources include high-voltage power-line discharge and computer-generated noise in electric motors.

Other noises include

- Generation–recombination noise: due to free carriers being generated and recombining in semiconductor material. They are random and can be treated as a shot noise process.
- Temperature fluctuation noise: the result of the fluctuating heat exchange between a small body, such as a transistor, and its environment due to the fluctuations in the radiation and heat conduction processes.

9. RECENT TRENDS

Figure 53 shows a 4-dB step, 28-dB variable attenuator for a 1.9-GHz personal handy phone system transmitter fabricated using silicon bipolar technology with f_T of 15 GHz. The GaAs MESFET variable attenuator is configured with resistive pi attenuators and GaAs switches as shown. Step accuracy within 1.2 dB and total vector modulation error of less than 4% were realized for −15 dBm output. The attenuator consumes 21 mA with 2.7 V power supply and occupies 1.1 × 0.5 mm. This unit is being developed. This shows the technology trend.

Figure 54 shows the top view and cross section of a prototype optical microwave attenuator that can be

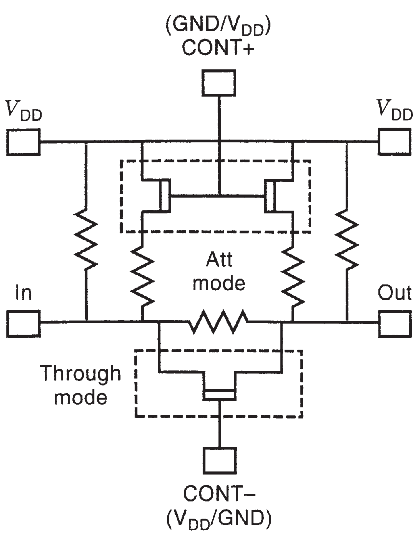

Figure 53. Variable attenuator using GaAs MESFET CONT+/CONT− = VDD/GND in attenuation mode and CONT+/CONT− = GND/VDD in through mode.

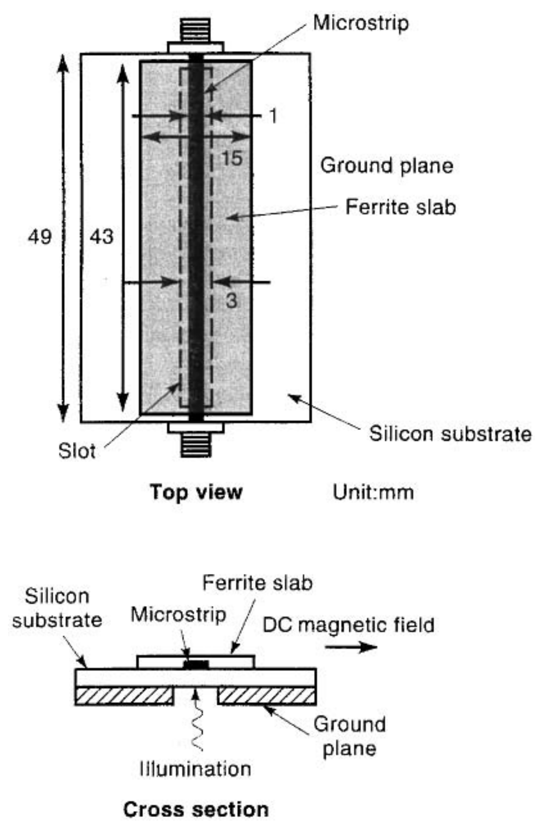

Figure 54. Microstrip–slotline attenuator on a silicon substrate with an override ferrite slab.

controlled by illuminating the silicon substrate. The maximum attenuation is 30 dB using laser diode illumination. It is a microstrip line whose substrate consists of silicon and ferrite slabs. The ferrite slab is overlaid on the microstrip. There is a slot on the ground plane under the strip. A white light from a xenon arc lamp with a parabolic mirror is focused by a lens to the silicon surface through the slot. The intensity of the light is not uniform along the slot direction. Due to the light, electron–hole pairs are induced and the permittivity and conductivity of the silicon are changed, which vary the phase and amplitude of the microwave. With 240 mW optical power illumination, an attenuation in the range of 17–26 dB was obtained in the frequency range from 8 to 12 GHz.

FURTHER READING

F. G. Ananasso, A low phase shift step attenuator using PIN diode switches, *IEEE Trans. Microwave Theory Tech.* **MTT-28**(7) (July 1980).

P. S. Bochert, *FET Attenuator, 0–1 GHz Applied Microwave and Wireless*, spring 1996.

R. G. Brown et al., *Lines, Waves, Ana Antennas*, Ronald Press, New York, 1973.

R. S. Elliot, *An Introduction to Guided Waves and Microwave Circuits*, Prentice-Hall, Englewood Cliffs, NJ, 1993.

Engineering staff of the Microwave Division, *Microwave Theory and Measurements*, Hewlett-Packard Co., 1962.

S. C. Harsany, *Principles of Microwave Technology*, Prentice-Hall, Englewood Cliffs, NJ, 1997.

M. R. Haskard, *Thick Film Hybrids—Manufacture and Design*, Prentice-Hall, New York, 1988.

Hewlett-Packard Application Note 1048, *A Low-Cost Surface Mount PIN Diode π Attenuator*, Hewlett Packard Co., 1996.

Hewlett-Packard Application Note 922, *Applications of PIN Diodes*, Hewlett Packard Co., 1997.

IEEE Std 474-1973, *Specifications and Test Methods for Fixed and Variable Attenuators, DC to 40 GHz*.

T. Koryu Ishii, *Microwave Engineering*, Harcourt Brace Jovanovich, New York, 1989.

J.-Y. Kim and R. L. Geiger, MOS active attenuators for analog ICS and their applications to finite gain amplifiers, *Proc. IEEE Int. Symp. Circuits and Systems*, 1994.

J.-Y. Kim and R. L. Geiger, Performance Characterization of an active attenuator using two cascaded MOSFETS, *Proc. 36th Midwest Symp. Circuits and Systems*, 1993.

J.-Y. Kim and R. L. Geiger, Characterization of linear MOS active attenuator and amplifier, *Electron. Lett.* **3**(7) (March 30, 1995).

J.-Y. Kim and R. L. Geiger, An inverting MOS active attenuator for monolithic applications, *Proc. Midwest Electro-Technology Conf.* 1993.

T. S. Laverghetta, *Practical Microwaves*, Prentice-Hall, Englewood Cliffs, NJ, 1996.

R. LaVerne Libbey, *Video Attenuator Using a Multiplier and FET*, a publication of RCA, New Jersey, 1975.

RF Microdevices, RF 2420 Programmable Attenuator Data Sheet, 1997.

RF & Microwave Test Accessories Catalog, Hewlett-Packard, 1997/98.

RF Microdevices Technical Application Note TA 0027, *Integrated, Single Step, 10 dB Attenuator for Power Control Applications*, 1997.

RF Microdevices, RF 2421, *10 dB Switched Attenuator Data Sheet*, 1997.

MIL-HDBK-216, military handbook, *R. F. Transmission Lines and Fittings*, Section 14, Attenuators, Nov. 1976.

MIL-A-3933E, military specification, *Attenuators, Fixed, General Specification for 1985*.

MIL-A-3933E, Suppl. 1, military specification, *Attenuators, Fixed, General Specification for 1985*.

S. Otaka et al., A 1.9 GHz Si-bipolar variable attenuator for PHS transmitter, *IEEE J. Solid State Circuits* **32**(9):1424–1429 (Sept. 1997).

Reference Data for Radio Engineers, 1957, International Telephone and Telegraph Corp., New York.

P. A. Rizzi, *Microwave Engineering—Passive Circuits*, Prentice-Hall, Englewood Cliffs, NJ, 1988.

D. Roddy, *Microwave Technology*, Prentice-Hall, Englewood Cliffs, NJ, 1986.

S. E. Saddow and C. H. Lee, Scattering parameter measurements on optoelectronic attenuator, *IEEE MIT-S Digest* (1994).

H. W. Sams, *Reference Data for Radio Engineers*, 7th ed., 1985, Indianapolis, IN.

G. E. Schafer and A. Y. Rumfelt, Mismatch errors in cascade-connected variable attenuators, *IRE Trans. Microwave Theory Tech.* (1959).

H. Shimasaki, S. Matsuda, and M. Tsutsumi, Phase compensation in an optically controlled microwave attenuator, *IEEE MTT-S Digest* 1703–1706 (1997).

V. A. Suprynowicz, *Electrical and Electronics Fundamentals—an Applied Survey of Electrical Engineering*, West Publishing, New York, 1987.

V. F. Valey, *Modern Microwave Technology*, Prentice-Hall, Englewood Cliffs, NJ, 1987.

A vector attenuator for feedforward amplifier and RF predistortion use, product features, *Microwave J.* (Oct. 1997).

Weinschel Associates Catalogue, *Attenuators and Terminations*, 1998.

R. E. Ziemer and W. H. Tranter, *Principles of Communications—Systems, Modulation, and Noise*, Wiley, New York, 1988.